NOVEMBER, 1970 REPORT R-497 UILU-ENG 70-242

CSL COORDINATED SCIENCE LABORATORY

MULTIPLE STATES AND VARIABLE INTENSITY IN THE PLASMA DISPLAY PANEL

WILLIAM DOOLEY PETTY

UNIVERSITY OF ILLINOIS – URBANA, ILLINOIS

UILU-ENG 70-242

MULTIPLE STATES AND VARIABLE INTENSITY IN THE PLASMA DISPLAY PANEL

by

William Dooley Petty

Principal support for this work was given by the Naval Air Development Center under Contract N2269-69-C-0013; auxiliary support was given in part by the Advanced Research Projects Agency (monitored by the U.S. Army Electronics Command) under Contract DAAB-07-67-C-0199; in part by the Joint Services Electronics Program (U.S. Army, U.S. Navy and U.S. Air Force) under Contract DAAB-07-67-C-0199; in part by a grant from Owens-Illinois, Incorporated.

MULTIPLE STATES AND VARIABLE INTENSITY IN THE PLASMA DISPLAY PANEL

William Dooley Petty, Ph.D.
Department of Electrical Engineering
University of Illinois, 1970

The development of the computer based educational system at the University of Illinois necessitated the investigation of economically feasible display units for use in student terminals. After existing display systems were examined, research was undertaken which, it was believed, would lead to a more satisfactory display. The result of this research was the invention of the plasma display panel in 1964 by Bitzer, Slottow, and Willson.

In its normal operation the plasma panel exhibits a bistable range in which the cells can exist in either of two stable modes. The "on" state results from a discharge every half cycle, and the "off" state corresponds to no discharges. This investigation is concerned with the attainment of multiple stable states with corresponding multiple intensities. The application of this technology is related most directly to computer output displays where the inherent memory of the multiple states is desirable.

The basic ideas upon which this research was initiated were set forth by Petty with the observation of stable discharge sequences which, when perturbed, had a slow return to equilibrium, and by Slottow who first developed a stability theory which explained this transition sequence. The basic stability theory was examined and predictions about device behavior were made to verify the theory. Based on device measurements and Slottow's theory, knowledge of plasma panel physics was extended with subsequent refinements of measurement techniques and device predictions. An

extended stability theory was later proposed and tested. Based on this knowledge, techniques were developed for maintaining the plasma display panel in three stable states.

TABLE OF CONTENTS

LIST OF FIGURES

CHAPTER 1.

Introduction

1.1 Background

The development of the computer based educational system (PLATO) at the University of Illinois necessitated the investigation of economically feasible display units for the use in student terminals. After existing display systems were examined, research was undertaken which, it was believed, would lead to the development of a more satisfactory display. The result of this research was the invention of the plasma display panel at the University in 1964 by Bitzer, Slottow, and Willson. The panel is a digitally addressable display with internal memory. The brightness is comparable to that of a cathode ray tube, and the projected cost is considerably less than that of a CRT with associated memory elements. In addition to its envisioned use in the PLATO system, the plasma panel is also well suited as a computer input-output device, a computer memory, and if it proves possible to introduce an appropriate gray scale and color, commercial television.

The plasma display panel consists of three dielectric elements with sets of parallel electrodes placed orthogonally on the outside dielectric as shown in figure 1.1. The central dielectric is a gas which will break down under the application of sufficient voltage. The outer dielectrics insulate the resulting discharge from the electrodes so that the discharge current produces a voltage across the cell walls.

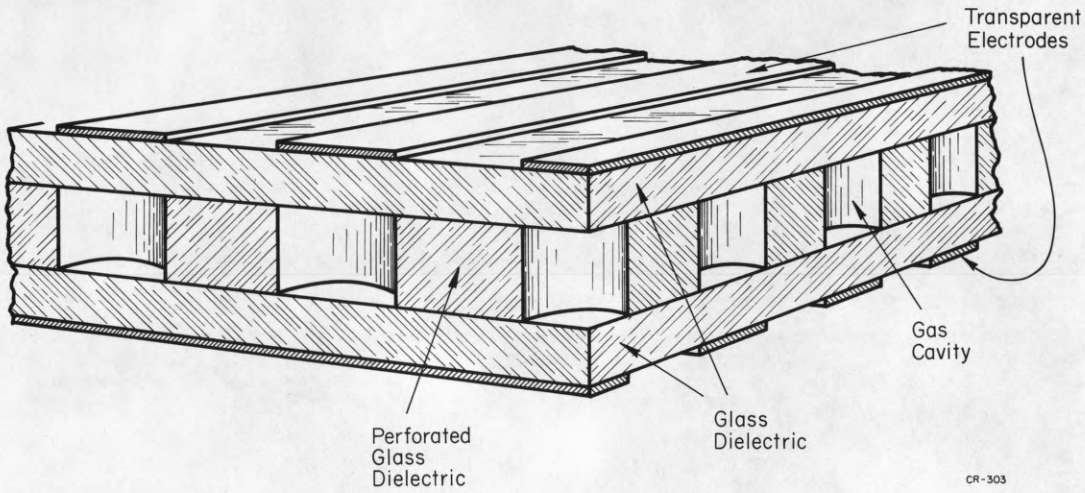

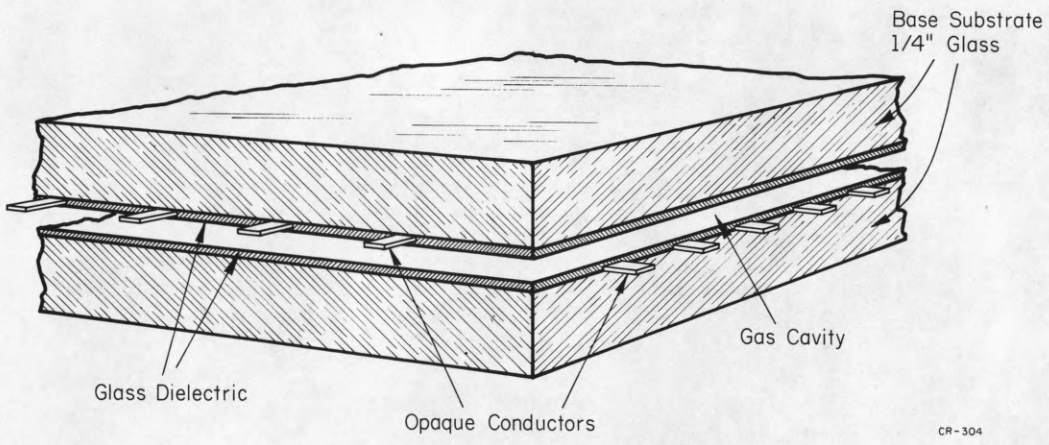

Figure 1.1
Plasma Display Panel Construction

Small panels with up to 1600 cells have been successfully fabricated at the University of Illinois. However, with the availability of quality plasma panels, under the brand name, Digivue, from Owens-Illinois of Toledo, Ohio, these have become the accepted standard. All measurements in this research project were made on a four inch square Digivue panel with a cell density of 33 cells/linear inch. Figure 1.2 shows a photograph of one of these panels.

In its normal operation the plasma display panel exhibits a bistable range in which the cells can exist in either of two stable modes. The "on" state results from a discharge every half cycle and the "off" state corresponds to no discharges. The current investigation is concerned with the attainment of multiple stable states in the plasma display panel with corresponding multiple intensities. The application of this technology is related most directly to computer output displays where the inherent memory of the multiple states is desirable.

The basic ideas upon which this research was initiated were set forth by Petty with the observation of stable discharge sequences, which, when perturbed, had a slow return to equilibrium, and by Slottow who first developed a stability theory which explained this transition sequence. The basic stability theory was examined and predictions about device behavior were made to verify the theory. Based on device measurements and Slottow's theory, knowledge of plasma panel physics was extended with subsequent refinements of measurement techniques and device predictions. An extended stability theory was later proposed and tested.

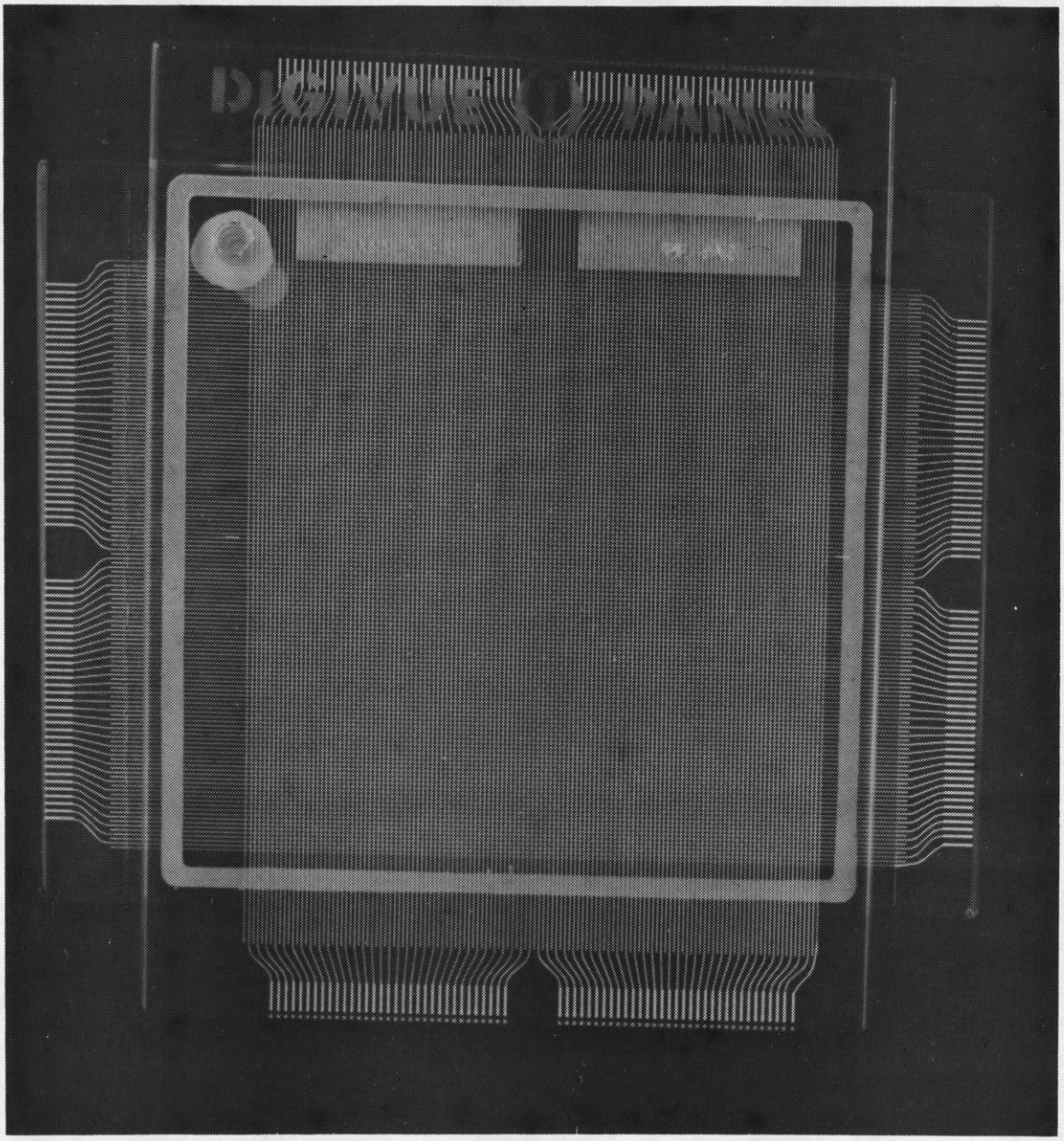

Panel Specifications: Type - Digivue
Matrix Size - 128 x 128 lines
Linear Density - 33 1/3 lines/inch
Structure Thickness - 0.5 inch

Figure 1.2
Digivue Panel from Owens-Illinois

Based on this knowledge, techniques were developed for maintaining the plasma display panel in three stable states.

1.2 Discharge Mechanism in the Plasma Panel

The plasma display cell, described physically in chapter 1.1, can be represented by the model shown in figure 1.3, where C_2 and C_3 represent the capacitance of the glass and C_1 represents the capacitance of the cell itself. The initial conditions on the cell are represented by the voltages V_1, V_2, and V_3. The current source I_D is the current of the discharge, and the source V_s is the externally applied source. The figure may be redrawn as shown in figure 1.4, in which all the information in the original model has been retained except that the capacitors C_2 and C_3 have been combined to form C_0 and the initial conditions have been represented externally. The voltage across the cell itself then is V_{ab}.

If V_S is equal to zero and no currents are present in the circuit then

$$V_{10} = V_{00} = V_W'$$

where V_{10} and V_{00} represent the initial voltages on capacitors C_1 and C_0 respectively.

$$V_S + V_W'\Big|_{t=t_o} - V_W'\Big|_{t=t_o} = \frac{1}{C_0}\int_{t_0}^{t_1} I_0 dt + \frac{1}{C_1}\int_{t_0}^{t_1} I_1 dt$$

in which

$$I_0 = I_1$$

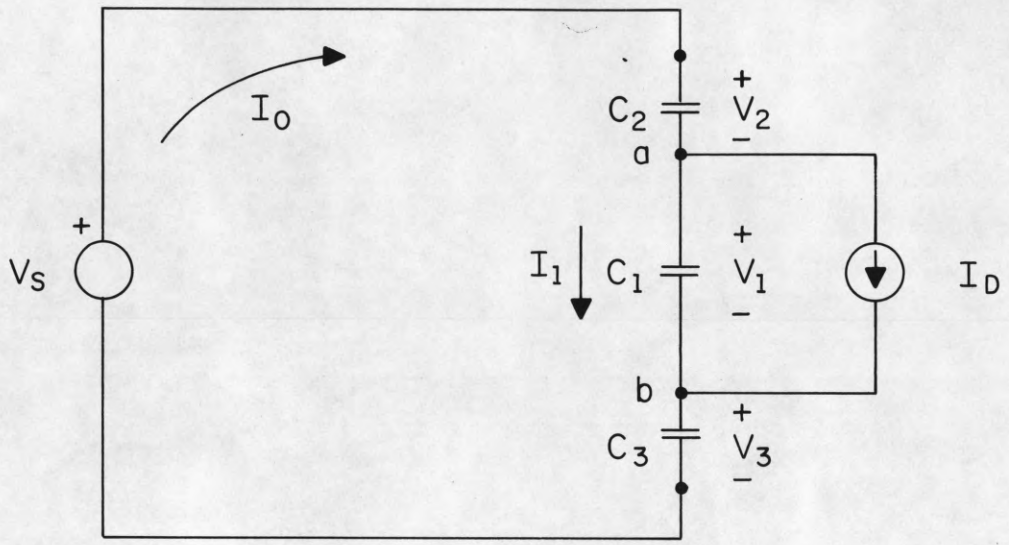

Figure 1.3
Equivalent Circuit Model of a Plasma Display Element

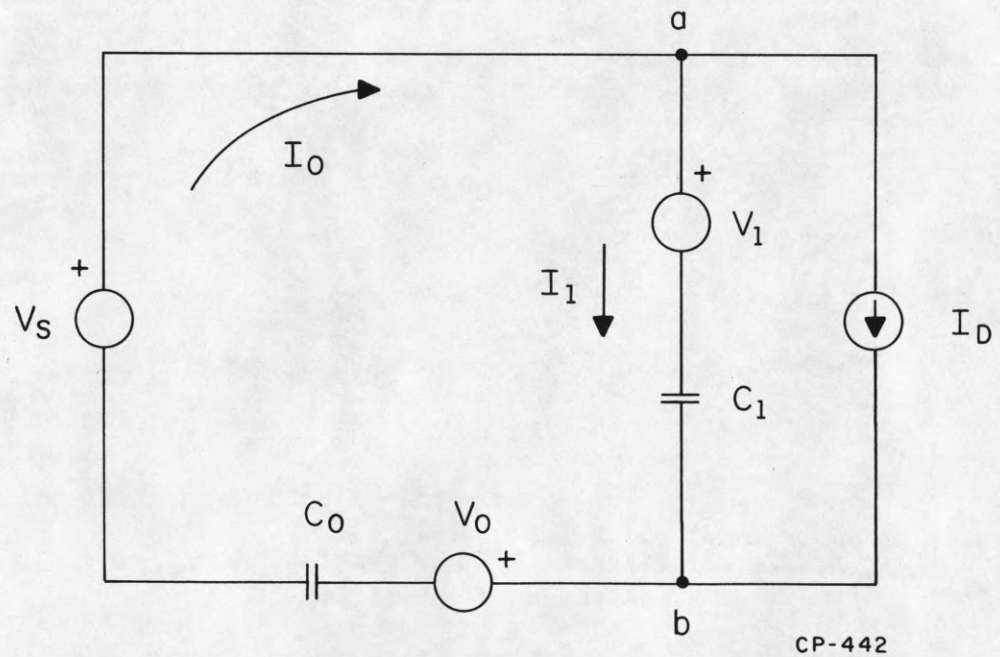

Figure 1.4
Simplified Circuit Model of a Plasma Display Element

or

$$V_{C1} = \frac{V_S/C_1}{1/C_1 + 1/C_0} = \frac{V_S C_0}{C_1 + C_0}$$

and

$$V_{ab} = V_W' + \frac{V_S C_0}{C_1 + C_0}$$

or

$$\left(\frac{C_1 + C_0}{C_0}\right) V_{ab} = V_S + \left(\frac{C_1 + C_0}{C_0}\right) V_W'$$

The terms in this equation are now referred to the outside of the panel rather than the cell itself, and for simplicity may be written as

$$V_C = V_S + V_W$$

Normally C_0 is much greater than C_1, so that

$$V_c \approx V_{ab} \qquad \text{and} \qquad V_W \approx V_W'$$

If V_S is sufficiently large so that a discharge occurs in the cell, then I_D is not zero and by superposition the effect of the current I_D

on the circuit can be derived independently of the voltage sources.

$$I_0 = \left(\frac{C_0}{C_1 + C_0} \right) I_D$$

$$I_1 = -\left(\frac{C_1}{C_1 + C_0} \right) I_D$$

and

$$V_{C1} = \frac{1}{C_1} \int_{t_0}^{t_1} I_1 dt = \frac{-1}{C_1 + C_0} \int_{t_0}^{t_1} I_D dt = \frac{-1}{C_0} \int_{t_0}^{t} I_0 dt$$

This value of V_{C1} caused by the discharge becomes the wall voltage V_W' at time t_1, so that

$$V_W\Big|_{t=t_1} = \left(\frac{C_1 + C_0}{C_0}\right) V_W'\Big|_{t=t_1} = -\left(\frac{C_1 + C_0}{C_0^2}\right) \int_{t_o}^{t} I_0 dt$$

Because C_0 is much greater than C_1

$$V_W \approx V_W' \qquad \text{and} \qquad I_0 \approx I_D$$

Throughout this report, all voltages given will be referred to the outside of the panel, e.g., the terms V_W, V_C, V_S, I_D will be used.

When the voltage across the cell (V_C) reaches a certain magnitude, defined as the breakdown voltage (V_B), a discharge occurs in the cell. The current thus produced, results in a charge buildup on the wall of the cell (V_W), which will completely or partially neutralize the applied

cell voltage. If the voltage applied is significantly below the breakdown voltage, there may be movement to the walls of any electrons in the gas at the time that the voltage is applied. However the resulting change in wall charge, ΔV_W, will be extremely small. If the voltage applied is below breakdown voltage, yet large enough that avalanches occur, then each succeeding avalanche will be smaller than the previous one and charge will be transferred, its magnitude being a function of the size of the first avalanche (or consequently upon the number of electrons present in the gas when the first avalanche was initiated), and the voltage which produced it. If the cell voltage is above the breakdown voltage, the successive avalanches grow in size until the total cell voltage is reduced below the breakdown voltage, at which time the avalanches diminish until the discharge extinguishes.

Thus the change in wall voltage can generally be expressed as a function of the number of electrons present in the gas and the magnitude of the applied cell voltage. However, the dependence of transferred wall charge upon the number of initial electrons diminishes rapidly for increasing V_C and the change in wall charge ΔV_W becomes a function of the cell voltage (V_C) at the time the discharge is initiated.

CHAPTER 2.

An Extended Stability Theory for Plasma Discharges

Slottow developed a theory for the stability of the plasma panel in which it is assumed that the change in wall voltage (ΔV_W) in a given discharge is a function of the applied cell voltage (V_C) at the time of the discharge. The results show that a discharge sequence is stable (i.e., if the wall voltage is perturbed from an equilibrium state, it will eventually return to that state provided that

$$0 < \frac{\partial \Delta V_W}{\partial V_{Ci}} \Bigg|_{V_{CO}} < 2$$

This approach to stability has been extended with the assumption that the panel is driven by a sequence of pulses, each of which may or may not in itself produce a discharge that satisfies the above criteria. Such a wave form is shown in figure 2.1.

If an arbitrary zero level (figure 2.2) is assumed, then in order for a series of discharges to form an equilibrium sequence the difference between the wall voltage and the zero level at the beginning of the sequence must be the same as the difference at the end of the sequence. To be stable the wall voltage in a set of such sequences must eventually return to its equilibrium state if perturbed by a small amount at any point in the sequence.

If the parameters of figure 2.3 are assumed, where "i" is the sequence number and "j" is the pulse number in that sequence, then the sequence is

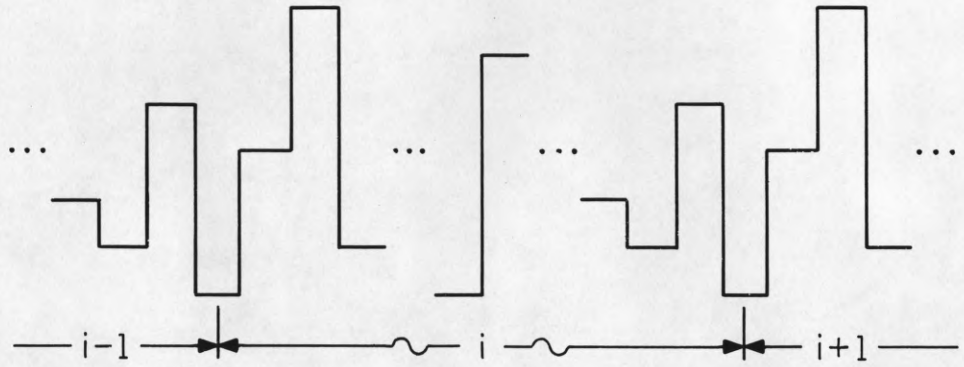

Figure 2.1
Hypothetical Sustaining Wave Form for a Plasma Panel

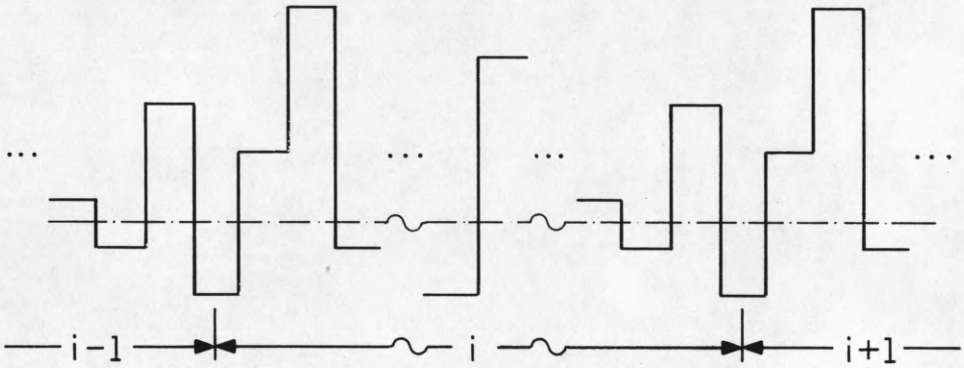

Figure 2.2
Sustaining Wave Form with Arbitrarily Selected Zero Level

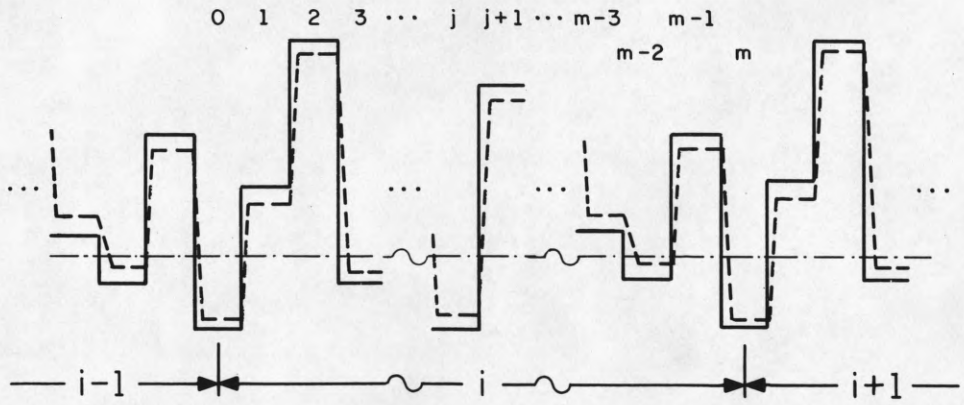

CP-443

Figure 2.3
Sustaining Wave Form with Representation of Wall Voltage

stable if

$$\left|\delta_{(i+1)j}\right| < \left|\delta_{ij}\right|$$

where δ_{ij} represents the difference between a given wall voltage and the corresponding equilibrium wall voltage after the "jth" discharge of the "ith" sequence. If an arbitrary pulse is selected as the beginning of a sequence, then this relationship becomes

$$\left|\delta_{(i+1)0}\right| < \left|\delta_{i0}\right|$$

The equilibrium wall voltage level at each pulse in a sequence is V_{WO}, V_{W1}, ... V_{Wj}, ... $V_{Wm} = V_{WO}$, the voltage of each pulse of the sustaining signal is V_{SO}, V_{S1}, ... V_{Sj}, ... $V_{Sm} = V_{SO}$, and the actual wall voltage at each pulse in the "ith" sequence is V_{Wi0}, V_{Wi1}, ... V_{Wij}, ... $V_{Wim} = V_{W(i+1)0}$. Assume that

$$V_{Wij} = f_j(V_{Wi(j-1)}, V_{Sj})$$

which for a constant value for V_{Sj} becomes

$$V_{Wij} = f_j(V_{Wi(j-1)})$$

Define the offset from an equilibrium wall voltage as

$$\delta_{ij} = V_{Wij} - V_{Wj}$$

Using the relationship expressed in the first two terms of the Taylor's series

$$f(x) = f(a) + f'(a)\ (x - a)$$

the following expression can be derived

$$V_{Wi(j+1)} = f_{j+1}(V_{Wij})$$

$$= f_{j+1}(V_{Wj}) + f'_{j+1}(V_{Wj})\ (V_{Wij} - V_{Wj})$$

$$= f_{j+1}(V_{Wj}) + f'_{j+1}(V_{Wj})\delta_{ij}$$

But

$$f_{j+1}(V_{Wj}) = V_{W(j+1)}$$

so

$$V_{Wi(j+1)} = V_{W(j+1)} + f'_{j+1}(V_{Wj})\delta_{ij}$$

or

$$V_{Wi(j+1)} - V_{W(j+1)} = f'_{j+1}(V_{Wj})\delta_{ij}$$

$$\delta_{i(j+1)} = f'_{j+1}(V_{Wj})\delta_{ij}$$

From this the entire sequence can be expressed.

$$\delta_{i1} = f_1'(V_{WO})\delta_{i0}$$

$$\delta_{i2} = f_2'(V_{W1})\delta_{i1}$$

.
.
.

$$\delta_{i(j+1)} = f_{j+1}'(V_{Wj})\delta_{ij}$$

.
.
.

$$\delta_{im} = f_m'(V_{W(m-1)})\delta_{i(m-1)} = \delta_{(i+1)0}$$

The combination of successive terms results in

$$\delta_{i1} = f_1'(V_{WO})\delta_{i0}$$

$$\delta_{i2} = f_2'(V_{W1})f_1'(V_{WO})\delta_{i0}$$

.
.
.

$$\delta_{i(j+1)} = f_{j+1}'(V_{Wj}) \cdots f_2'(V_{W1})f_1'(V_{WO})\delta_{i0}$$

.
.
.

$$\delta_{im} = f'_m(V_{W(m-1)}) \cdots f'_{j+1}(V_{Wj}) \cdots f'_1(V_{WO})\delta_{i0}$$

which can in turn be expressed as

$$\delta_{im} = \delta_{(i+1)0} = \left[\prod_{j=1}^{m} f'_j(V_{W(j-1)})\right]\delta_{i0}$$

Therefore, for equilibrium

$$V_{Wi0} = V_{W(i+1)0}$$

and for stability

$$\delta_{(i+1)0} < \delta_{i0}$$

or

$$-1 < \left[\prod_{j=1}^{m} f'_j(V_{W(j-1)})\right] < 1$$

where

$$f'_j(V_{W(j-1)}) = \frac{\partial V_{Wij}}{\partial V_{Wi(j-1)}}\bigg|_{V_{W(j-1)}}$$

This is graphically interpreted in figure 2.4 for a square wave. Note that by choosing the ordinate and abscissa as shown the derivative $f'_j(V_{Wi(j-1)})$ becomes the slope of the curve.

The development of the extended stability theory shows the combined effect of a sequence of discharges on a perturbation from equilibrium.

The nature of a typical discharge is a function of many variables, (e.g., the nature of the preceding discharge, the time since the preceding discharge, the number of metastables in the volume, the duration of the pulse

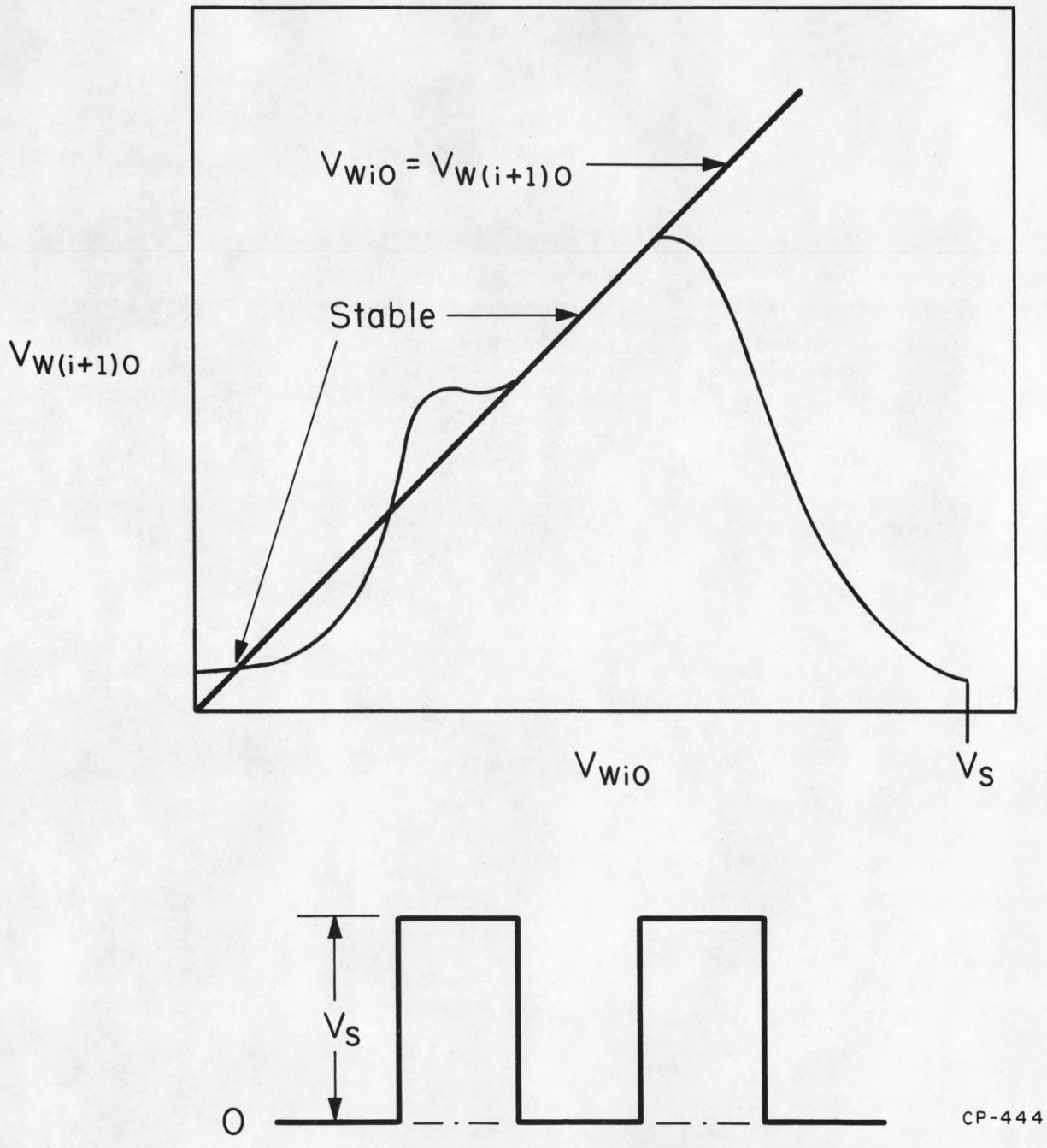

Figure 2.4
Representation of Stability Criteria

causing the discharge, the amplitude of the pulse, and the polarity of the applied voltage).

Typically the parameter used most frequently to describe a discharge is the maximum change in voltage across the cell as a function of the cell voltage. Because of the variables mentioned above this does not yield a complete picture of cell behavior but is useful for most applications, especially if a family of curves exists which takes the more significant functions into account.

Figures 2.5 through 2.8 show the effect of selected parameters upon ΔV_W using a 20 micro second pulse as a standard. Details of these measurements are given in Appendix A.

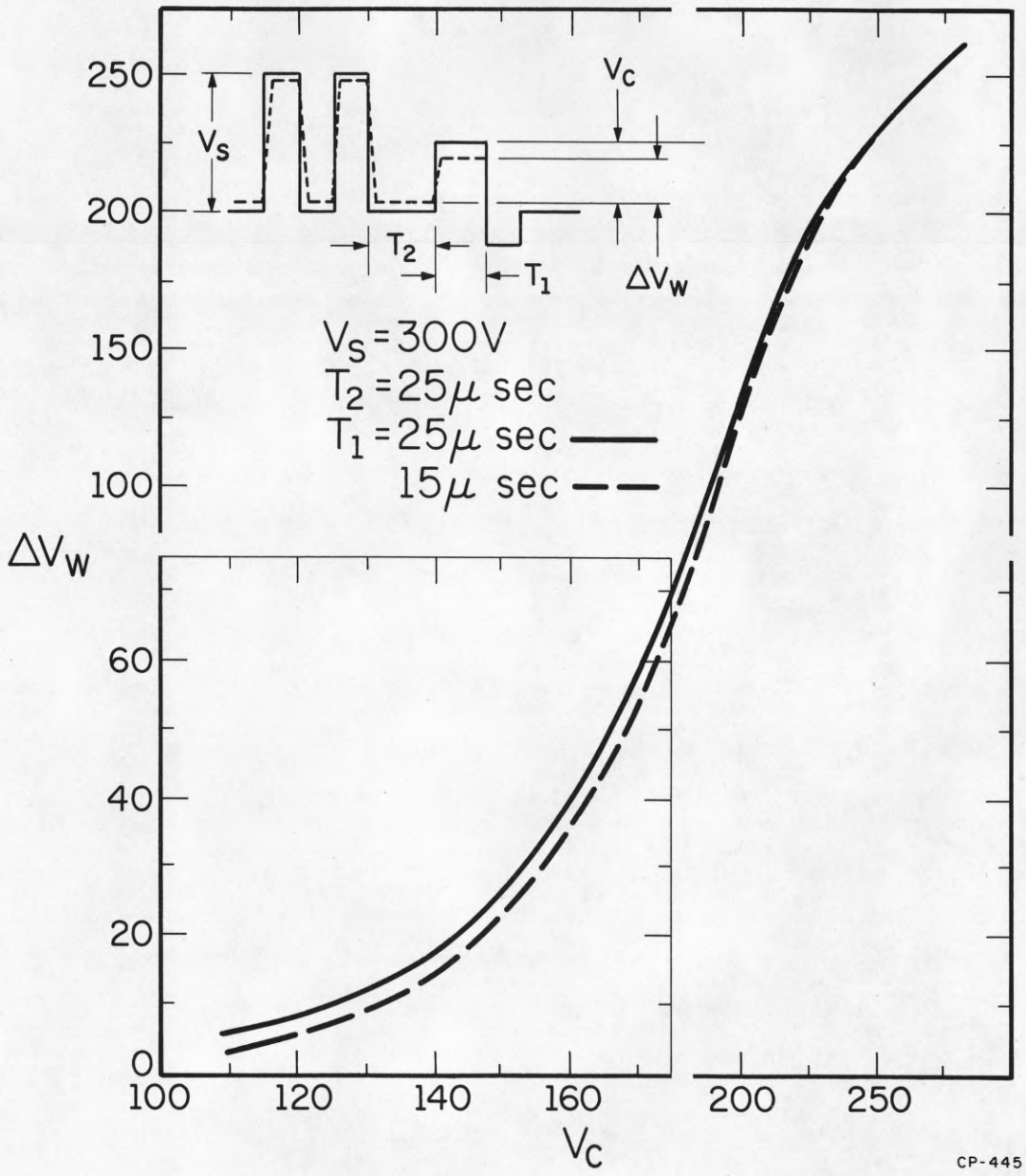

Figure 2.5
Wall Charge Transfer Characteristic as a Function of the Test Pulse Width

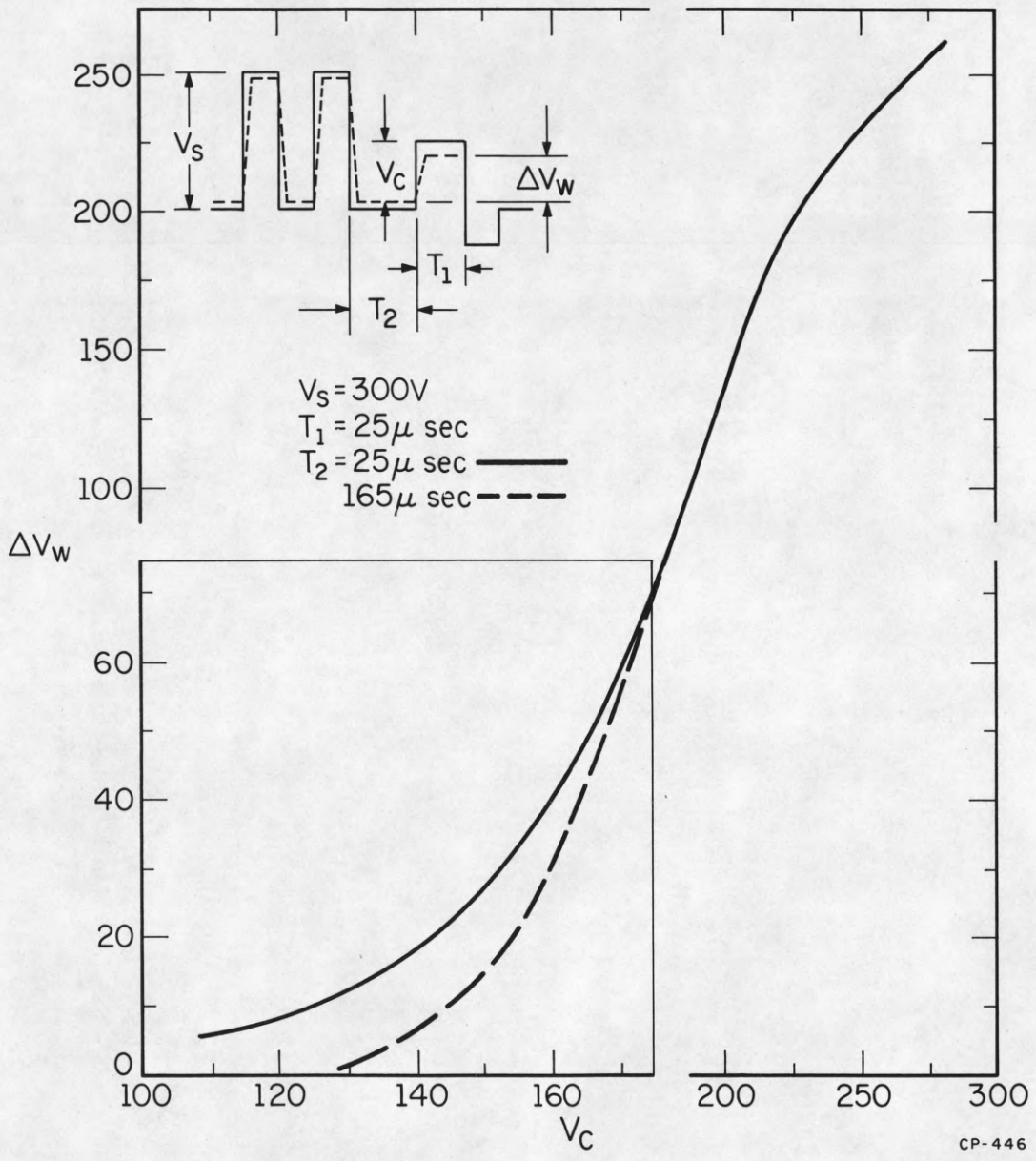

Figure 2.6
Wall Charge Transfer Characteristic as a Function
of the Time Between the Test Pulse and the Previous Discharge

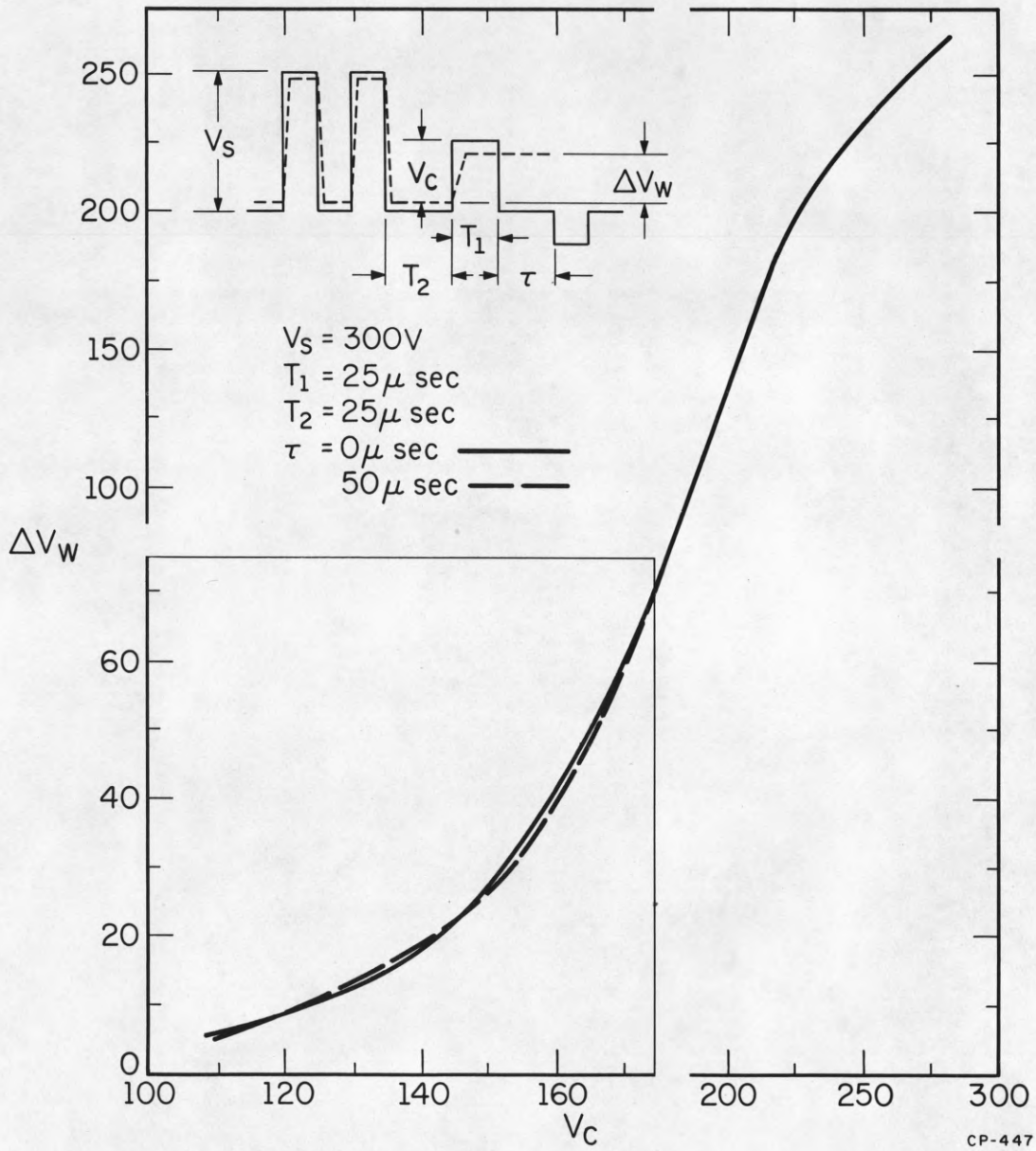

Figure 2.7
Wall Charge Transfer Characteristic as a Function
of the Time Between the Test Pulse and the Subsequent Discharge

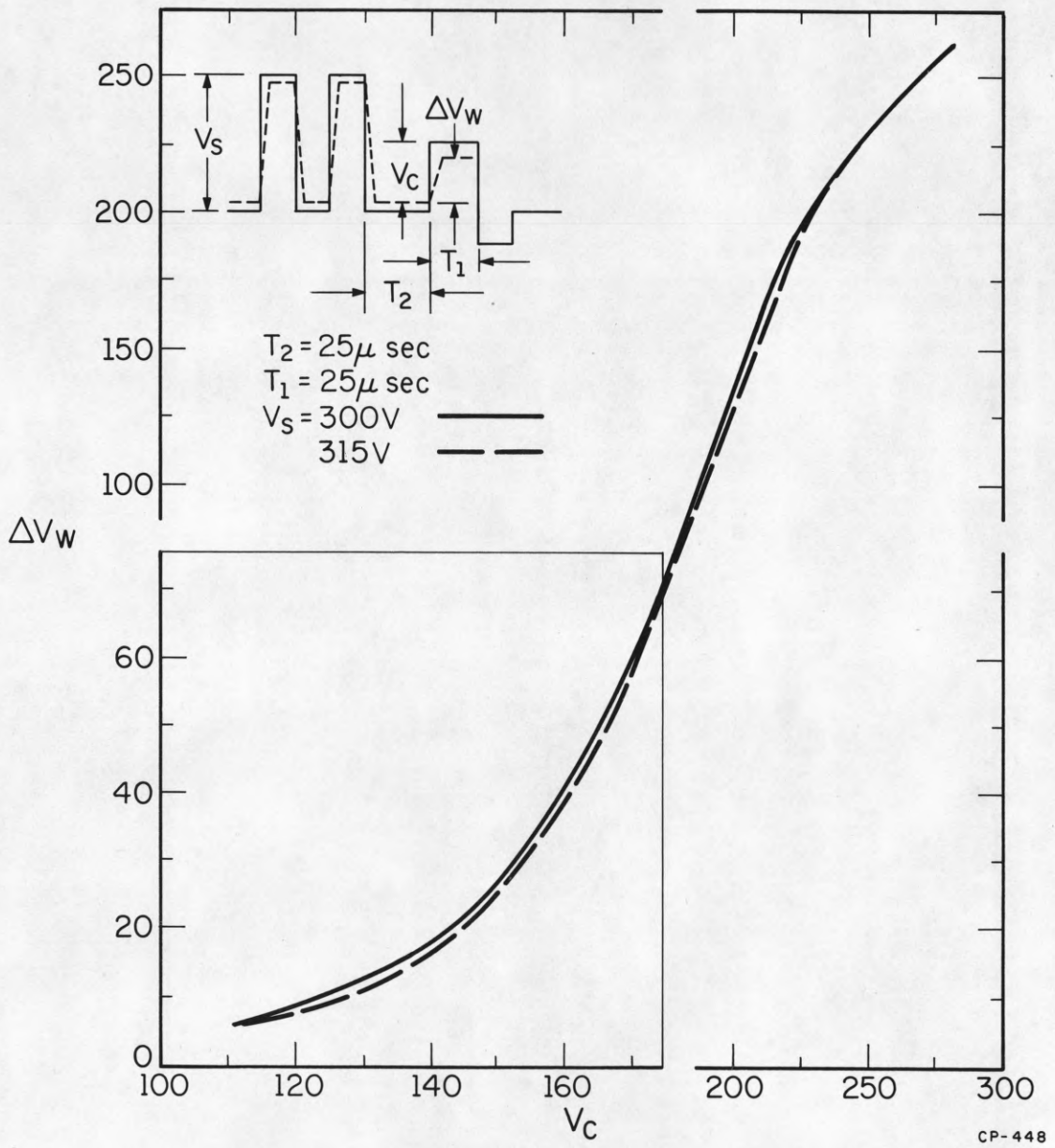

Figure 2.8
Wall Charge Transfer Characteristic as a Function
of the Amplitude of the Sustainer

CHAPTER 3.

Multiple Stable States

The cell characteristics described in the preceding chapter provide the information needed to obtain multiple stable states in the plasma display panel. It is necessary to vary the firing parameters so that there is more than one stable sequence of discharges for a given sustaining signal.

3.1 Two "On" States with a Square Wave Sustainer

The simplest means of achieving two stable states is by selecting a sustaining wave form designed from a consideration of the V_W versus V_C characteristic.

Although present techniques allow complete measurement of the V_C versus V_W curve, when measurements of these parameters were originally undertaken circuits which were available were capable of measuring only that portion of the characteristic shown in figure 3.1. The wave form of figure 3.2 was applied to the cell. A wall voltage equal to V_W existed on the cell at time t_1 as a result of V_S. The amplitude of V_A was adjusted until discharge activity was observed at time t_2. From this it was concluded that

$$V_F = V_W + V_A$$

which can be used to establish the functional relationship

$$\Delta V_W = 2V_W = 2(V_F - V_A) = f(V_C) = f(V_S + V_W)$$

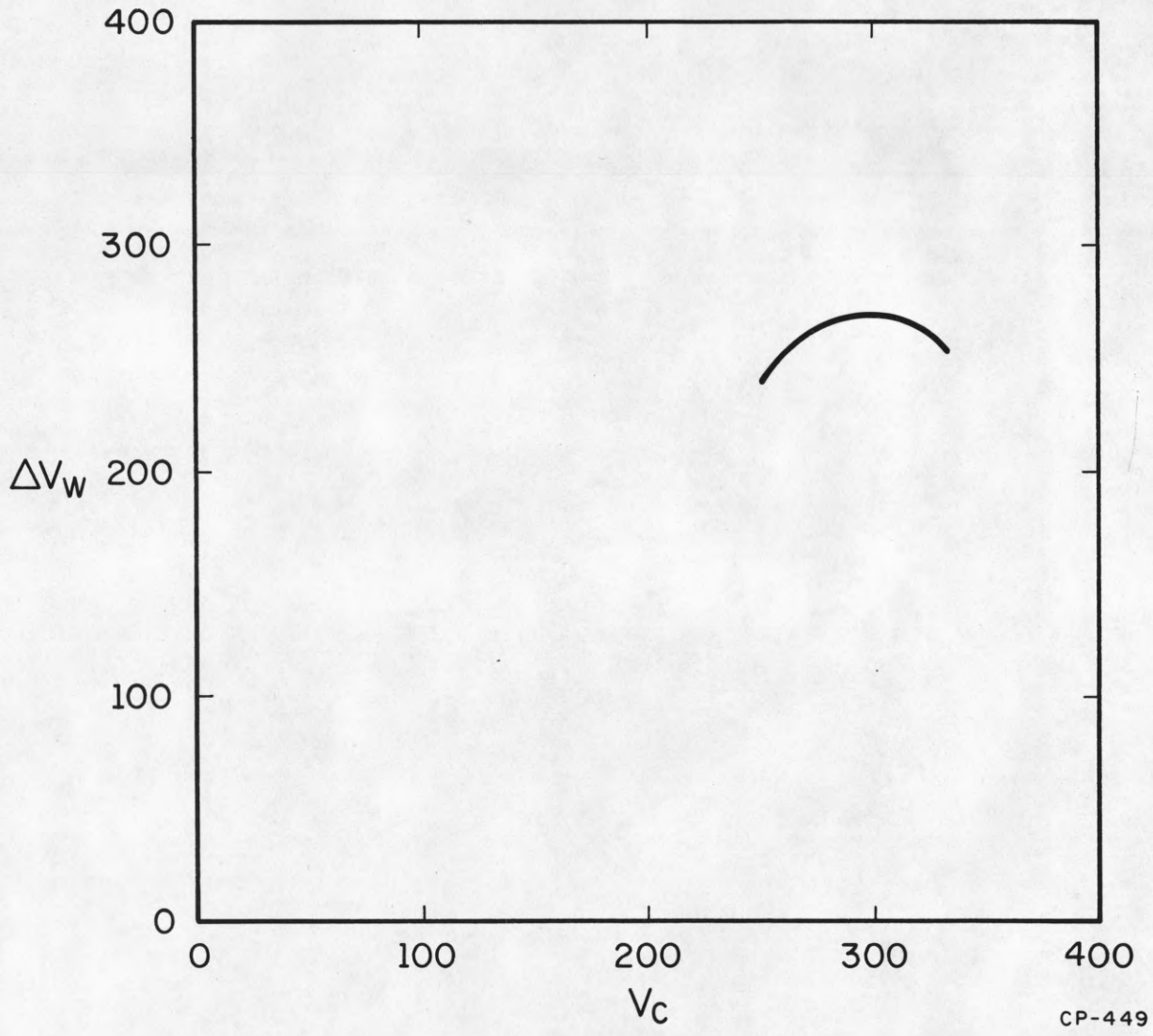

Figure 3.1
Wall Charge Transfer Characteristic for Equilibrium Condition

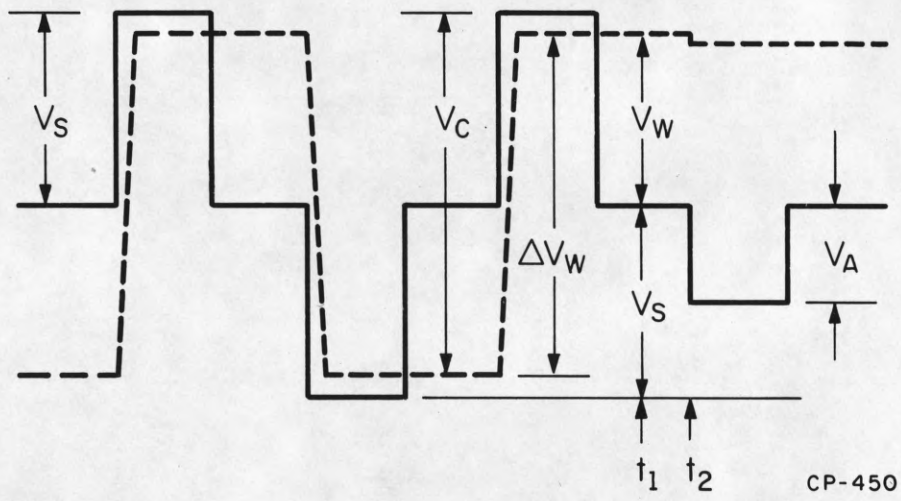

Figure 3.2
Wall Voltage Measurement Technique for Equilibrium Condition

The decrease in ΔV_W with increasing V_C for large values of V_C results from a second discharge that occurs at the trailing edge of the sustaining pulse as shown in figure 3.3.

Although not actually measured until later, it was proposed that the curve may become tangential to the horizontal axis at some time prior to intersection. If this should prove to be true, then Slottow's Stability Theory predicts that there must be a region in this lower portion which is stable, as shown in figure 3.4. The region at the right, where the slope becomes negative, should not be considered unstable, as it results from two discharges and Slottow's Theory considers only single discharges. Observations have shown this region to be stable.

If the V_W versus V_C characteristic of figure 3.4 is transposed to reflect a steady state sustaining signal in which

$$V_W = \Delta V_W/2$$

and

$$V_S = V_C - \Delta V_W/2$$

then the requirements for stability change from

$$0 < \frac{\partial \Delta V_W}{\partial V_C}\Big|_{V_{CO}} < 2$$

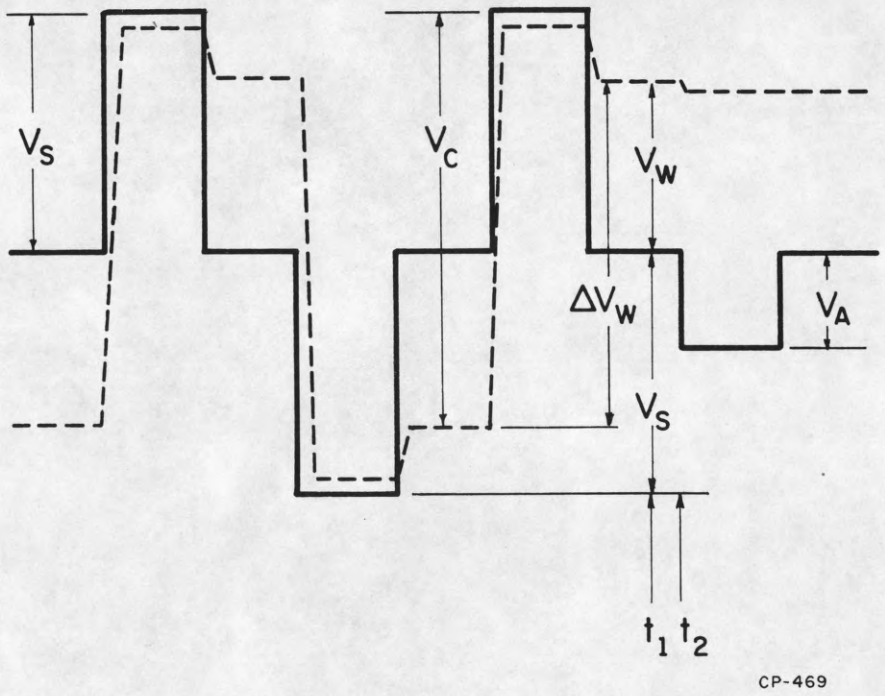

Figure 3.3
Effect of Discharge at Trailing Edge of Pulse
on Wall Voltage Measurements

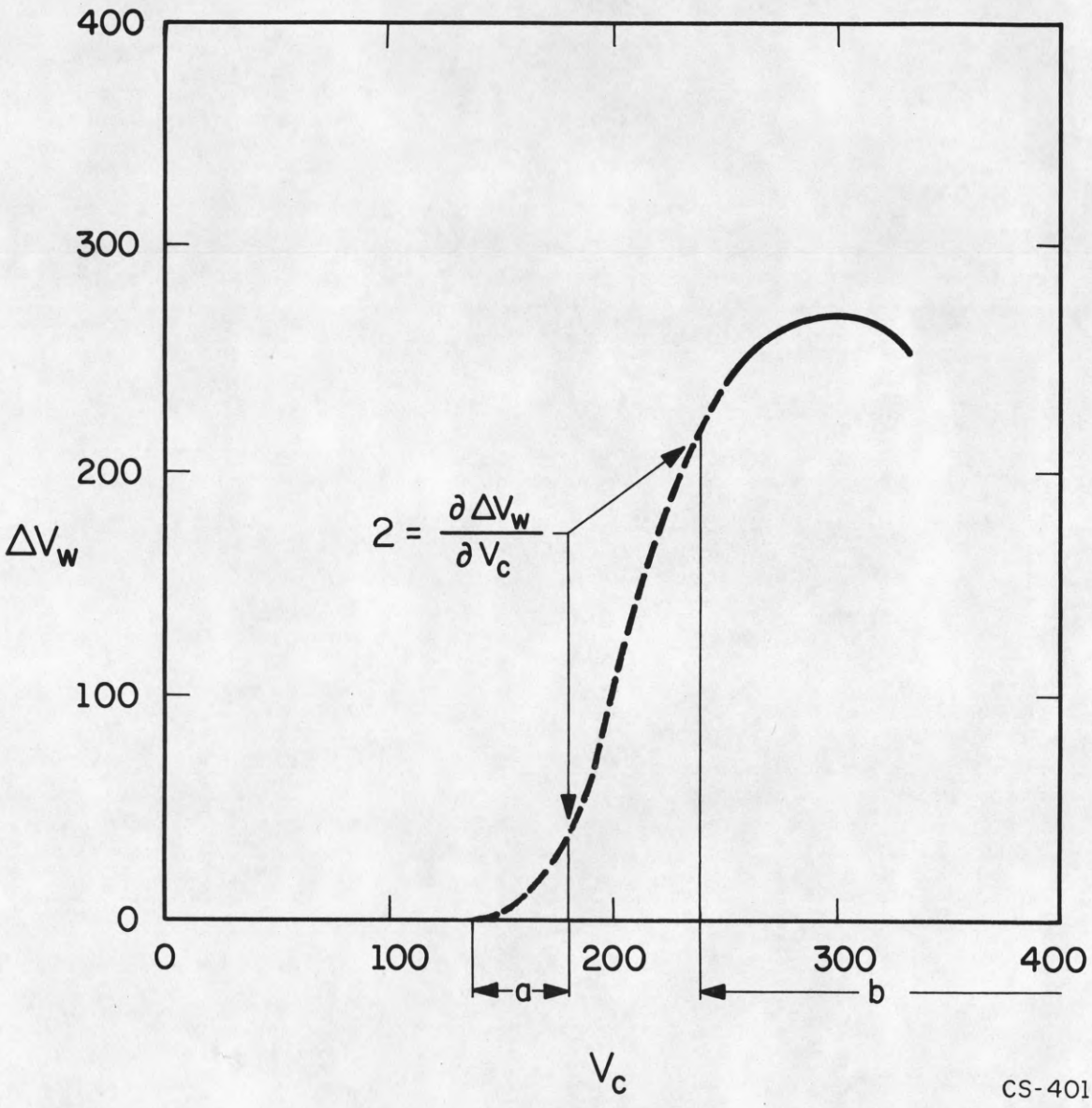

Figure 3.4
Proposed Extrapolation of Wall Charge Transfer Curve

to

$$\left.\frac{\partial V_W}{\partial V_S}\right|_{V_{SO}} > 0$$

It can be seen from figure 3.5, that in the region "a" to "b" there are two stable states for a fixed sustaining voltage (again the upper region with negative slope is not unstable). Attempts to find a second stable mode in this region using a square wave were successful. The curves of figure 3.6 establish the range of variation of the period for which the two states exist. Figure 3.7 shows the same information but extends it for non-square rectangular wave forms.

In measuring this set of curves the pulse width of the sustaining signal wave form was varied from two microseconds to T/2 and the results plotted. It was assumed that varying the pulse from T/2 to T would result in a mirror image of the obtained results. The curves of figure 3.7 form, in effect, third diemsnional cross sections of a generalized two state curve which considers all rectangular waves in which the square wave curve of figure 3.6 makes up the locus of central points.

3.2 Three States with a Square Wave Sustainer

The achievement of these two states lends credence to Slottow's Stability Theory as well as the hypothesis about the shape of the curve. However, the nature of the light pulse in the dim state (figure 3.8) was not as expected (i.e., it was not a simple complete discharge each half cycle).

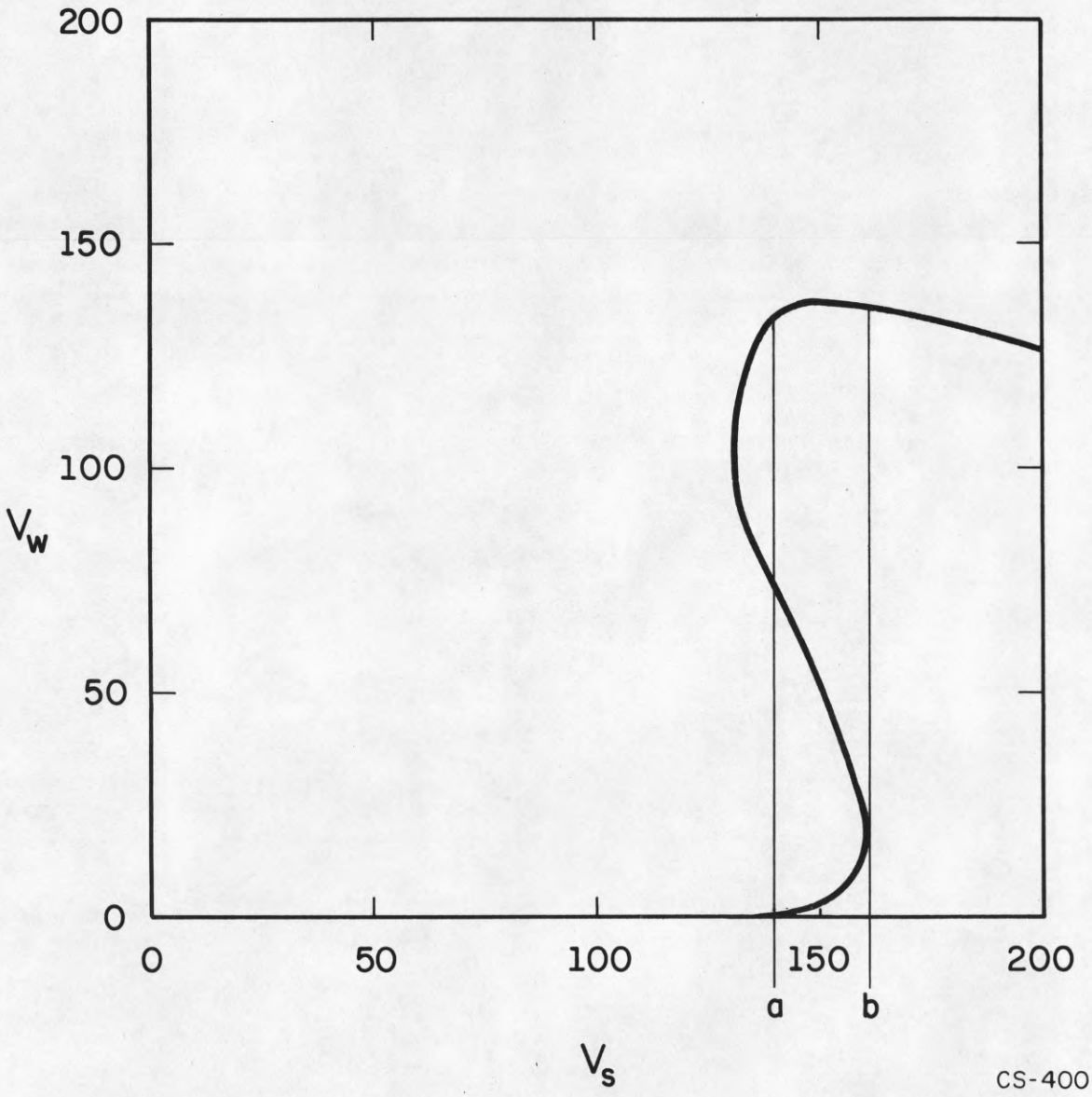

Figure 3.5
Wall Charge Characteristic Showing Bistable Range

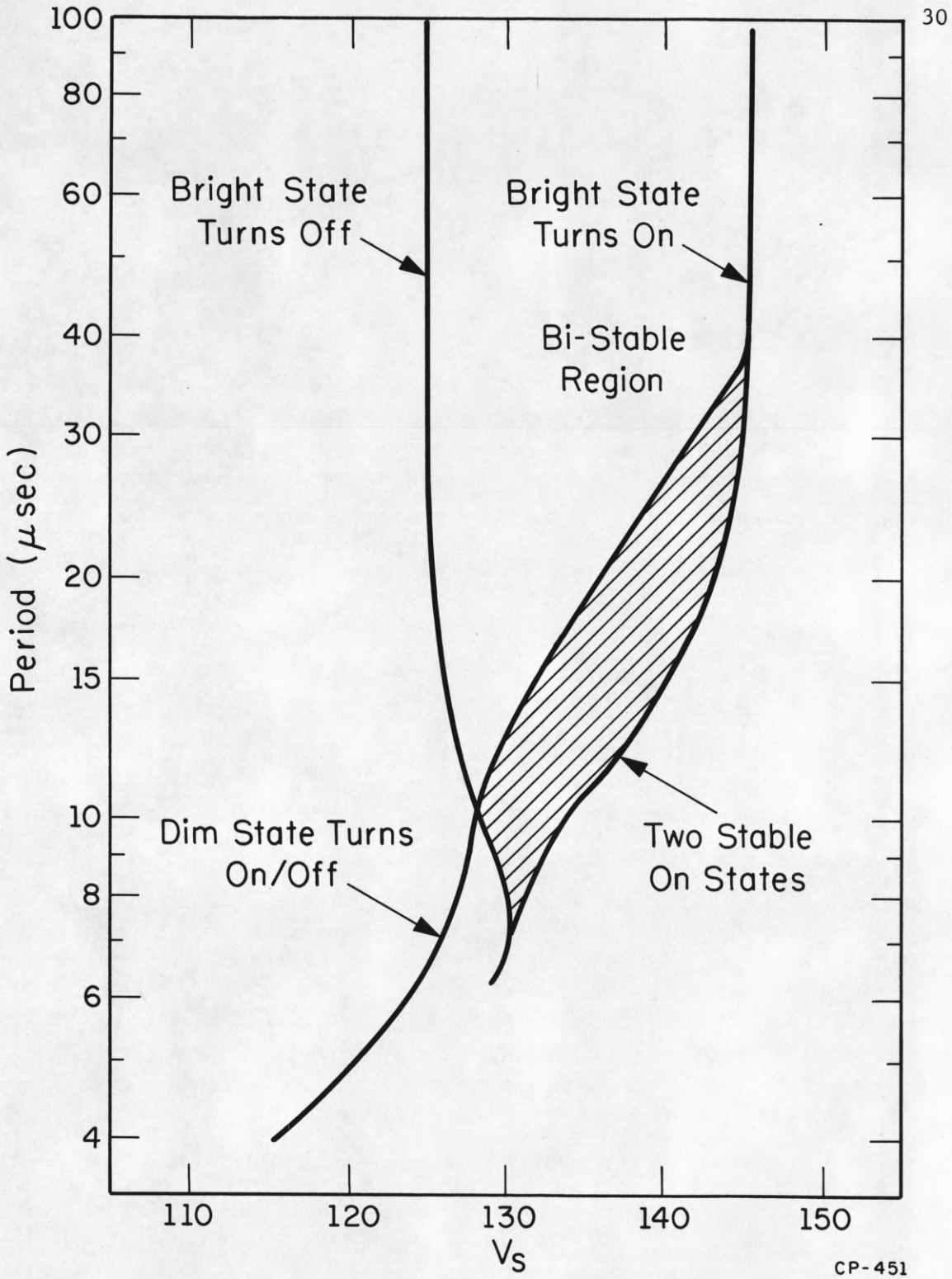

Figure 3.6
Bistable Voltage Range Represented as a Function
of the Period of a Square Wave Sustaining Signal

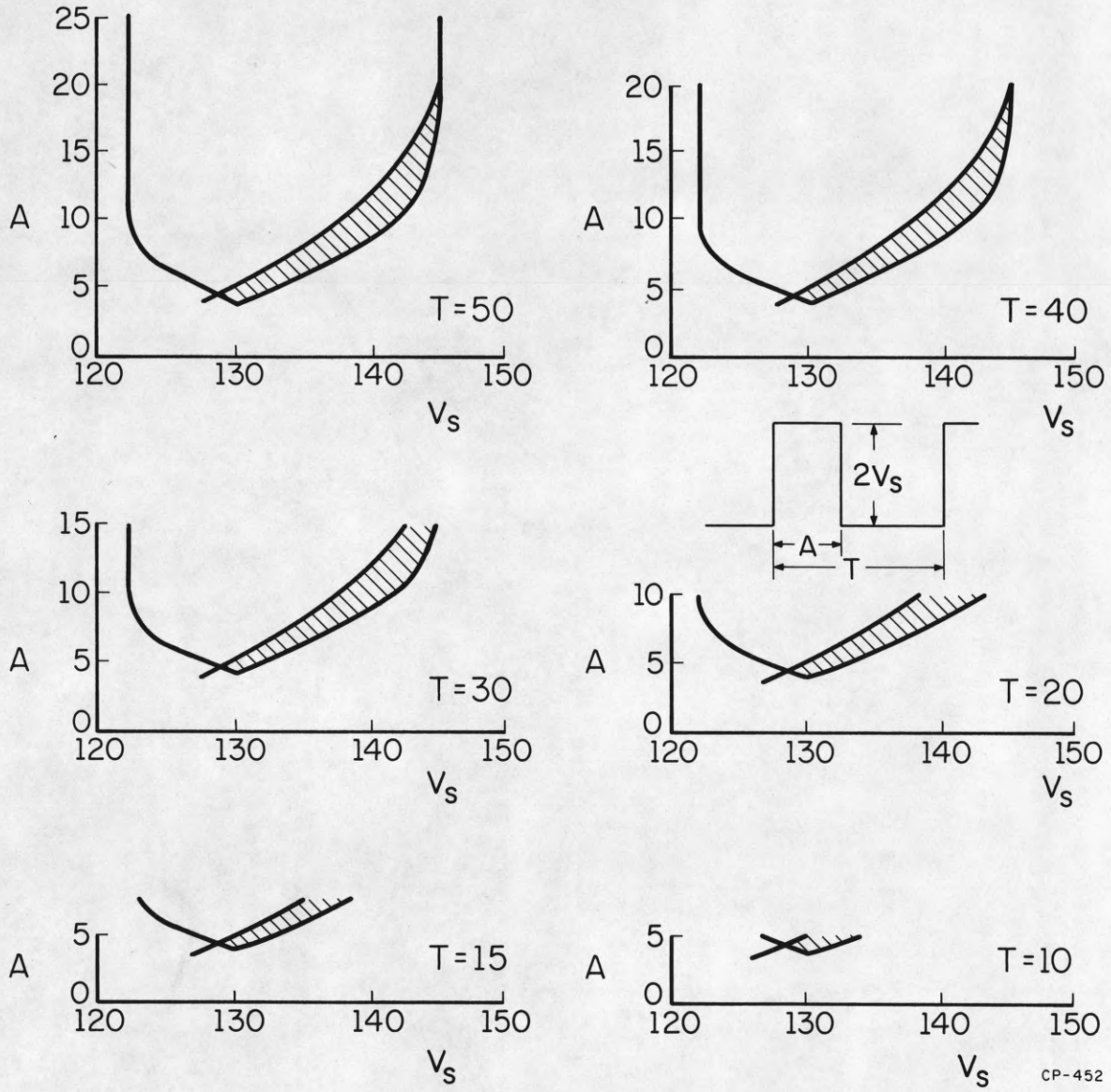

Figure 3.7
Bistable Voltage Range as a Function of the Pulse Width
for a Rectangular Wave Sustaining Signal

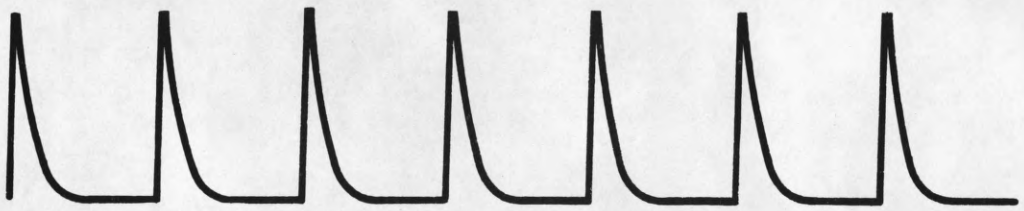

Light Output of Bright State

Light Output of Dim State

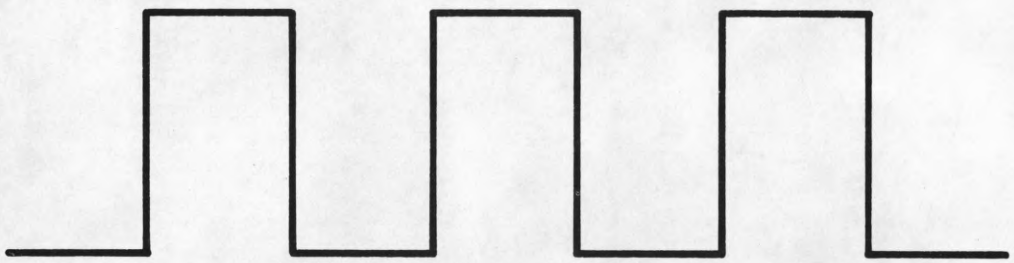

Sustaining Signal

CS-398

Figure 3.8
Light Output from Two "On" States Produced
with a Square Wave Sustaining Signal

Additional tests were performed with an extended range of sustainer to gain an understanding of these discharges. It was found that a cell could exist in two states with a rectangular sustaining signal (figure 3.9) provided that the pulse width (T_1) did not exceed about 20 microseconds and the complete period (T_2) did not exceed about 200 microseconds; the two times being independent. These observations led to an extended understanding of the role of the discharge process in establishing stable modes of operation.

The ability of the gas to sustain a discharge depends primarily upon the voltage across the cell (V_c) and the number of initiating electrons. These electrons are produced by the collision of metastables with the walls and after 200 microseconds the metastable population has been reduced to the point where there are insufficient electrons available to produce breakdown at the applied voltage of the pulse. For times less than 200 microseconds, the electron population is sufficient for a breakdown to occur. However, because of the low electron population density and the low cell voltage at the beginning of the short pulse, the avalanches build up slowly so that by the time the polarity of the applied signal is reversed the number of electrons and ions in the space is large. Although the cell voltage is then below breakdown, avalanches still occur. Each avalanche, however, is smaller than the preceding one, and the discharge extinguishes. The discharge activity results in a build up of the metastable population sufficient to carry on the sequence.

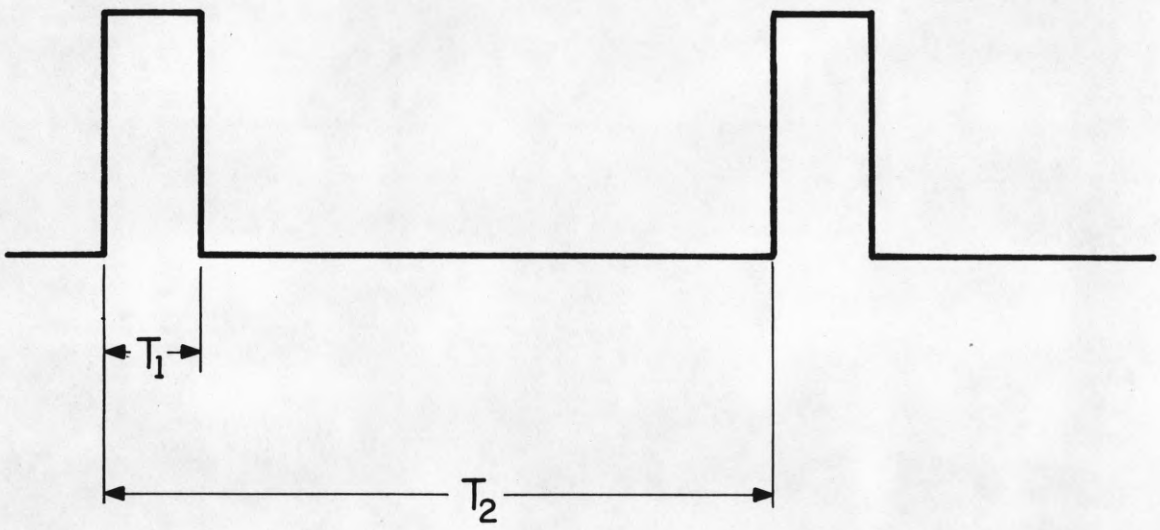

Figure 3.9
Sustaining Signal Parameters

These results clarified the role of repetitive sequences of discharges in multi-state modes, and stimulated the development of the extended stability theory explained in chapter 2.

The results also require an extension in the charge transfer description of cell behavior which accounts for the particles in the space. In figure 3.10, curve "a" represents the behavior of a cell in which there are relatively few electrons at the time a discharge is initiated. This corresponds to the leading edge of the pulse of figure 3.9. Curve "b" represents the response of a cell in which there is a great number of electrons at the time of a discharge, as on the trailing edge of the pulse in figure 3.9. Based on this information the hypothetical curve of figure 3.11 was used to explain the equilibrium of a cell in two "on" states. The bright state occurs because of the repeated application of the voltage

$$V_C = V_S + V_W = V_S + \Delta V_W/2$$

each half cycle resulting in change in wall voltage of $2V_W$. If only a small wall voltage is present, then, with the application of the sustaining pulse, the voltage V_A will exist across the cell causing a change in wall voltage as indicated. When the polarity of the sustaining signal is reversed the voltage across the cell is now V_B producing a discharge with associated change in wall voltage. For equilibrium this change in wall voltage must bring the cell voltage to the same level as at the start of the sequence.

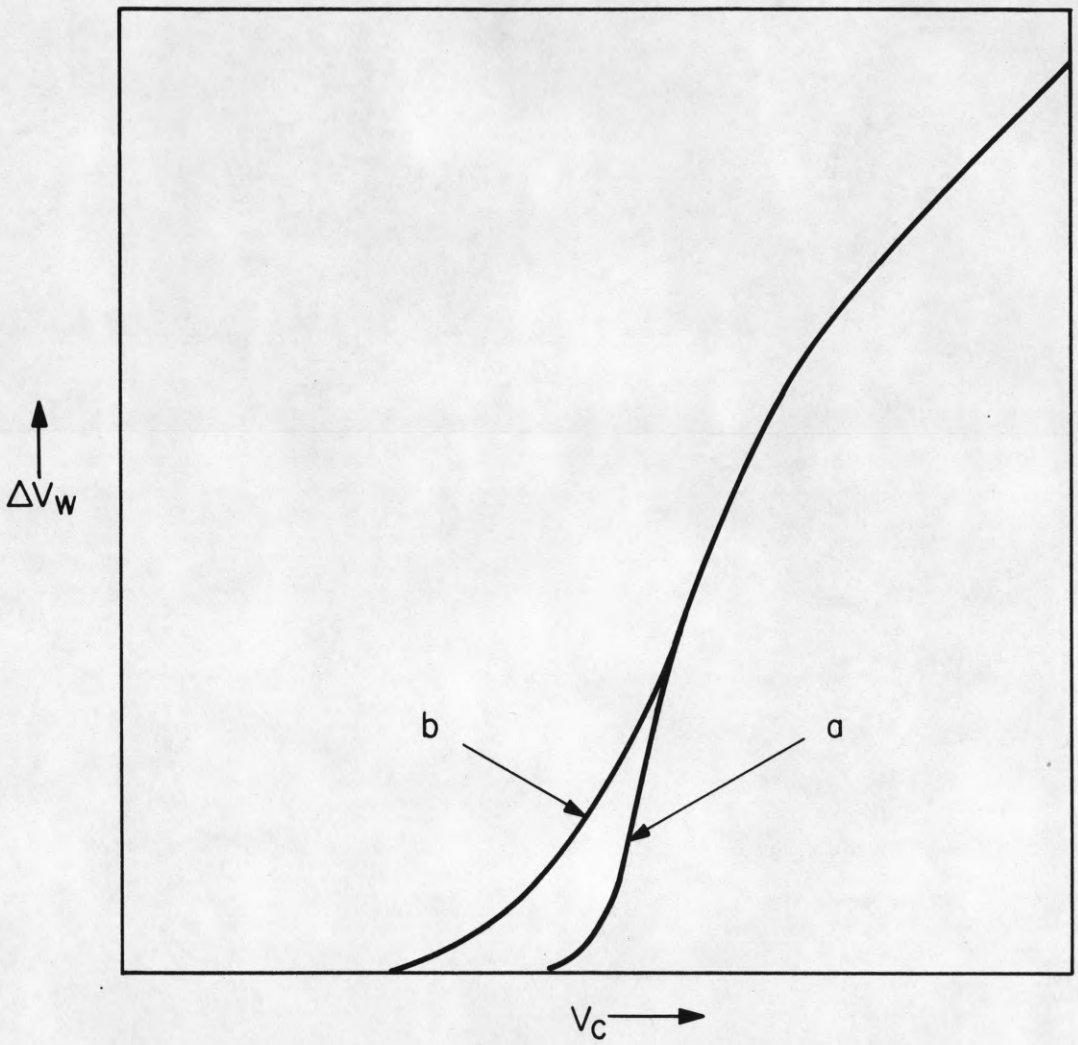

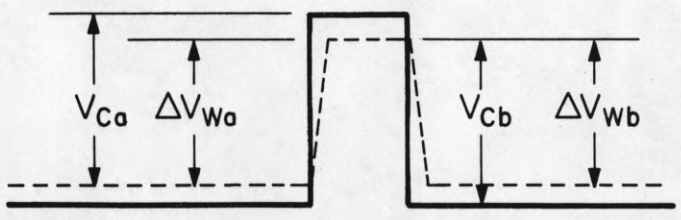

CP-453

Figure 3.10
Modified Wall Charge Transfer Curve

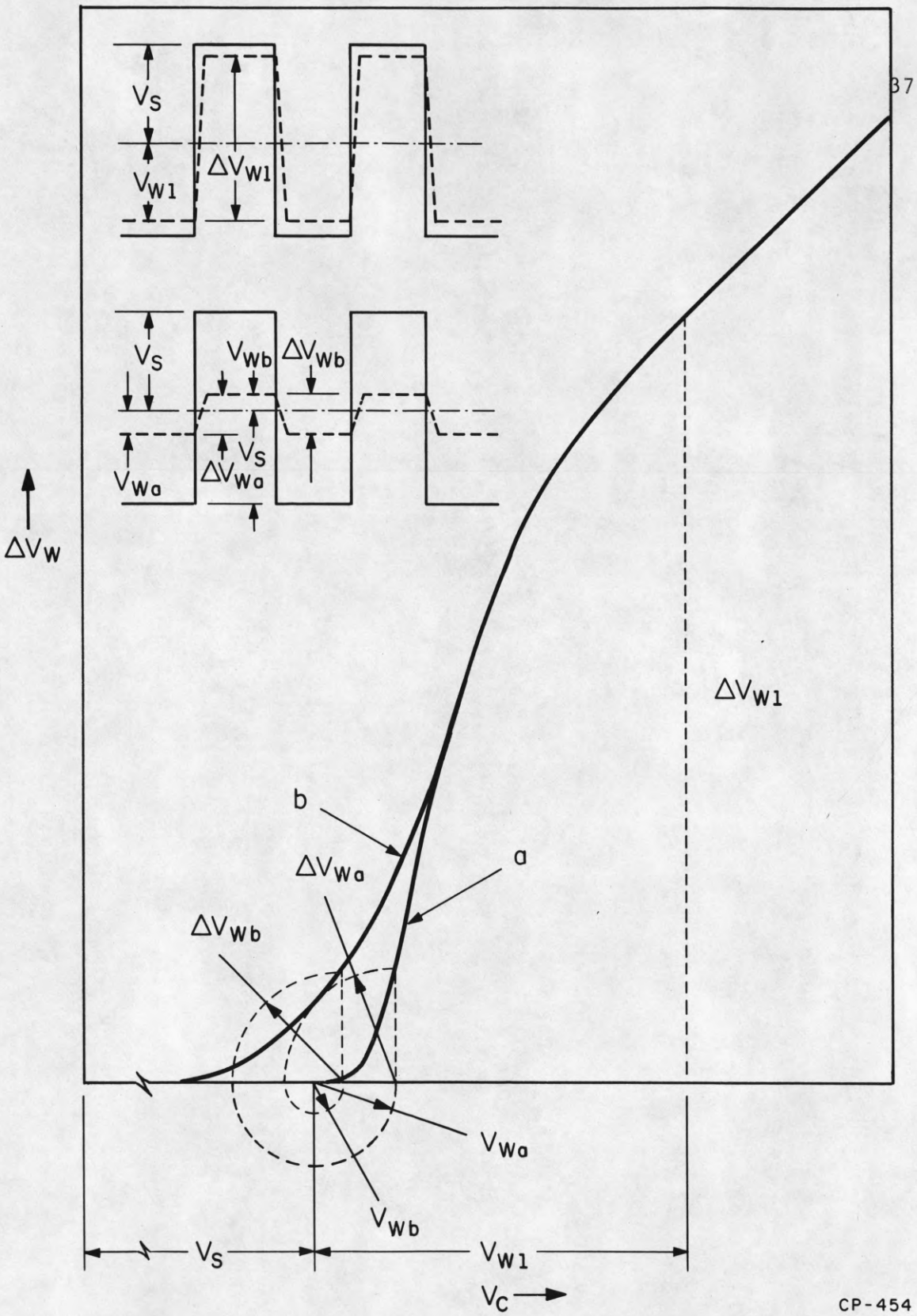

Figure 3.11
Achievement of Equilibrium States with a Square Wave Sustaining Signal

It was also noted that a sustaining signal with pulse height V_S with no initial wall voltage and no charges in the volume should produce no discharge. Consequently there should be three stable states, "bright", "dim", and "off". Attempts to observe the "off" state in coincidence with the other two states were successful. It was necessary to realize this state in an isolated section of the panel, however, in order to avoid the effect that charges in the space resulting from the other discharges would have on the cells under observation. This requirement eliminates this mode from any practical considerations.

The curves of figure 3.11 can be replotted to represent the functional relationship described in the generalized stability theory (figure 3.12) in which

$$V_{W(i+1)0} = V_{Wi0} + \Delta V_W \qquad \text{for } 0 \leq V_{Wi0} \leq 2V_S$$

where ΔV_W is found from the curve, letting

$$V_C = 2V_S - V_{Wi0}$$

Note that it is necessary to use curve "a" or curve "b" depending upon the condition in the cell when the voltage V_C is applied.

It can be seen that for the curve shown there are three stable states as indicated. The fact that these were observed lends support to the stability theory as well as to the hypothesis of the nature of the discharge.

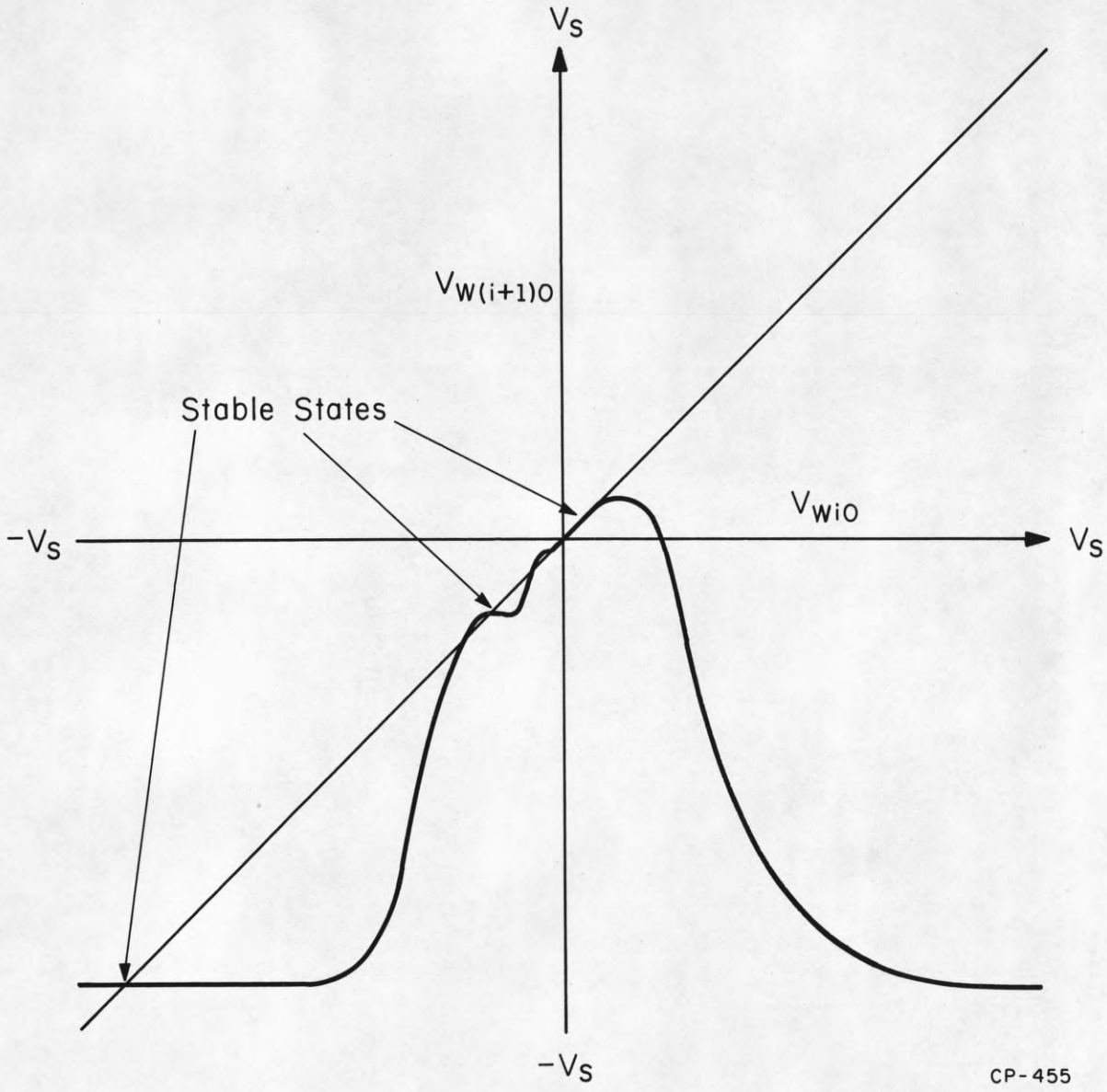

Figure 3.12
Graphical Representation of Stable Equilibrium States of Figure 3.11

3.3 Three "On" States

Three coincident stable states have been achieved using the multi-level square wave form of figure 3.13. A diagrammatic representation of the wall voltage is shown in figure 3.14. Because all of these are "on" states the problem of space charges from adjacent discharges does not create the problem that exists in the "off" state of the square wave sustainer. A photograph of a section of a panel in which these three states exist is shown in figure 3.15.

3.4 Multiple "On" States Using a Two Level Step Wave Form

Two stable states may also be achieved with the wave form of figure 3.16. Because of the difference in the widths of A and B a different amount of charge is deposited as a result of the respective discharges at the leading edge of A and of B. The light pulses are shown in figure 3.17, and a diagrammatic representation of wall voltage in figure 3.18.

It was observed also that two states could be achieved by allowing discharges twice each half cycle as shown in figures 3.19 and 3.20. However, in this particular case, three states were not obtained by combining the two techniques described because they occured for different width pulses. For narrow pulses the first bistable sequence was observed, while for wide pulses the second bistable sequence was observed (figure 3.21).

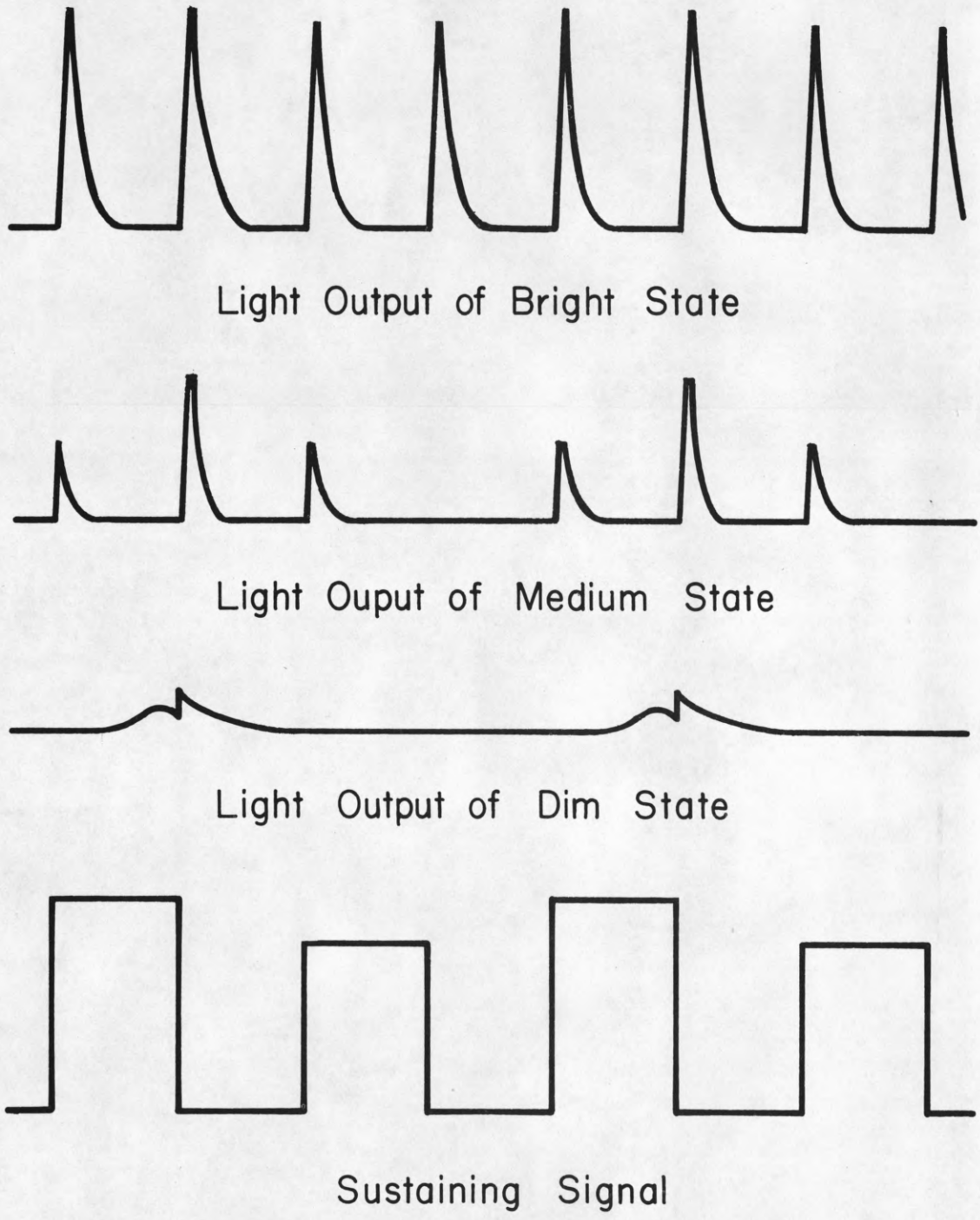

Figure 3.13 CS-402
Light Output from Three "On" States Produced with a Two Level Rectangular Wave Sustaining Signal

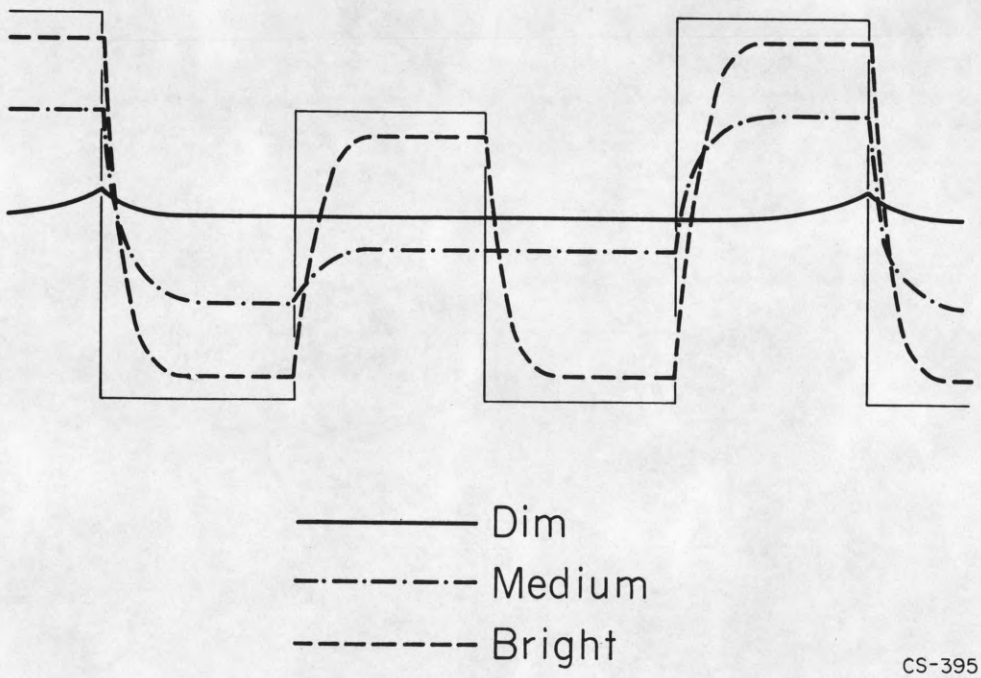

Figure 3.14
Representation of Wall Voltages from the
Three States of Figure 3.13

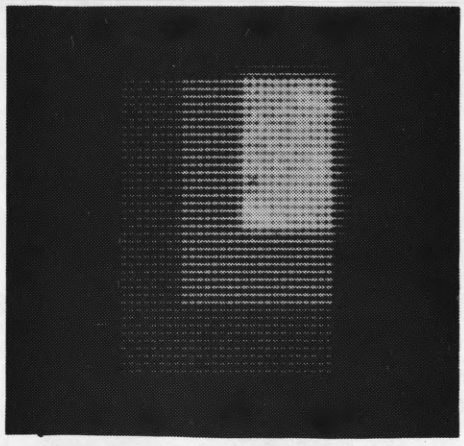

Figure 3.15
Three States Displayed on the Plasma Display Panel

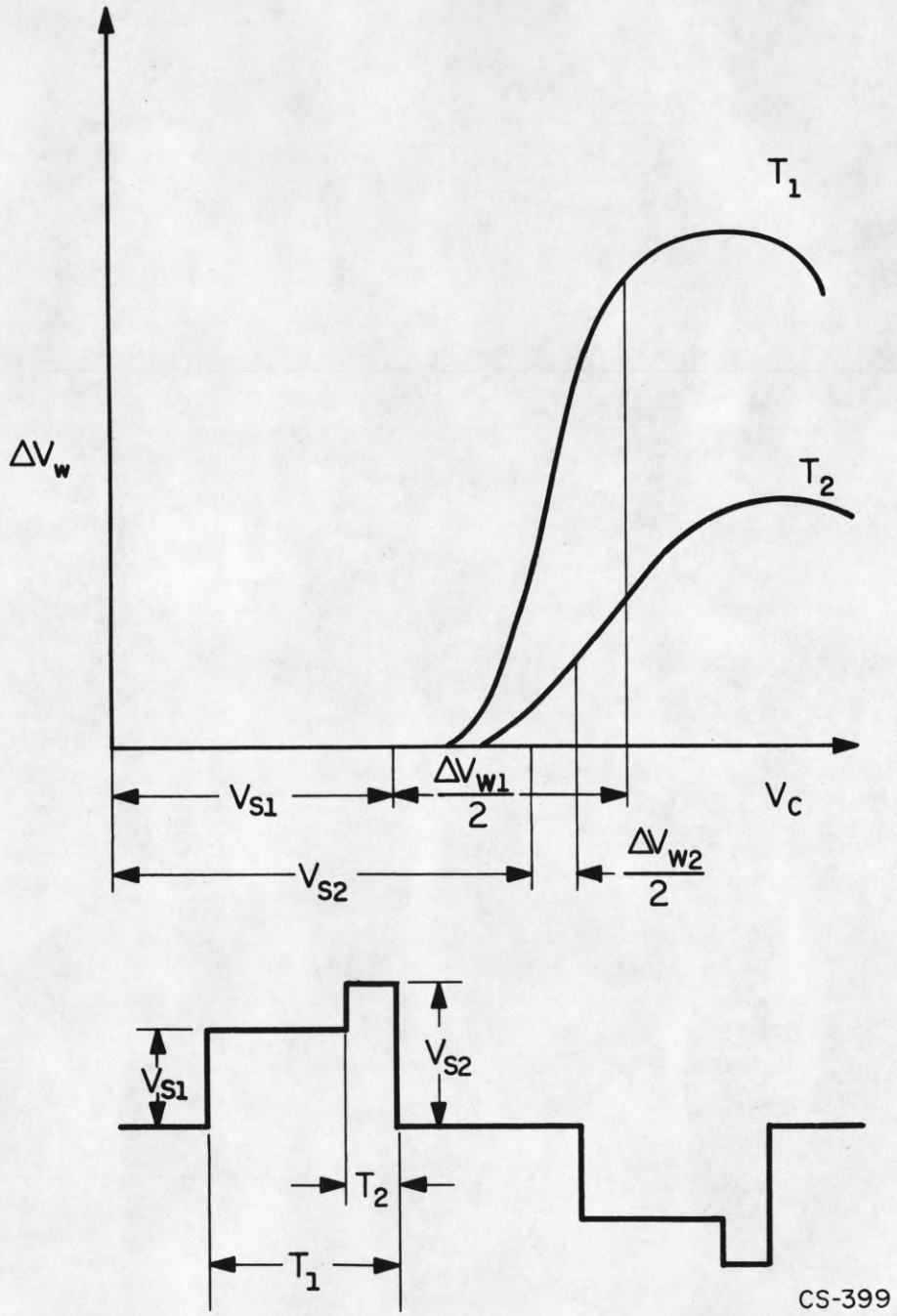

Figure 3.16
Achievement of Two States with a Stepped
Wave Form Sustaining Signal

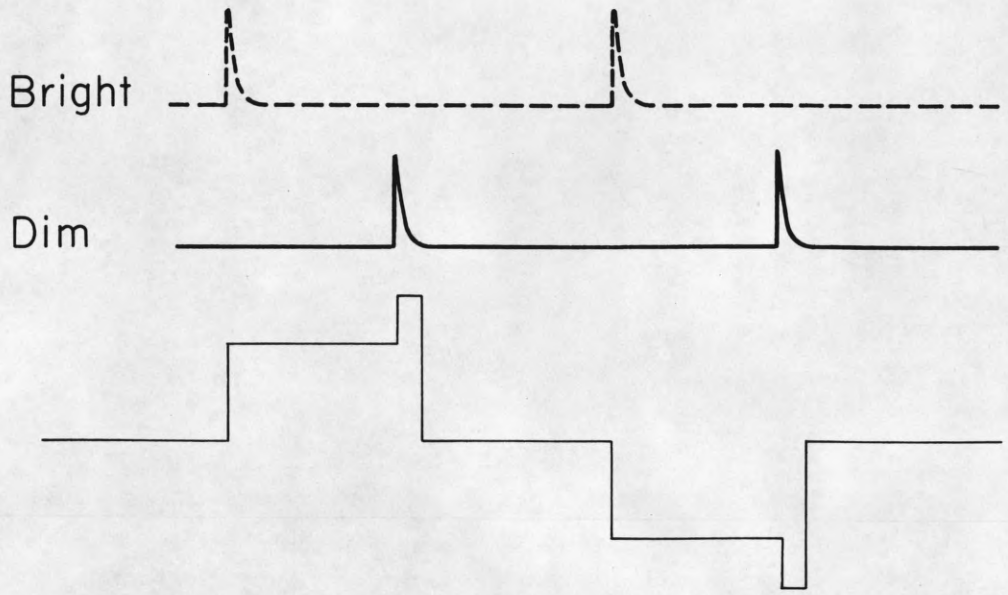

CS-397

Figure 3.17
Light Output of Two States with a Stepped
Wave Form Sustaining Signal (first mode)

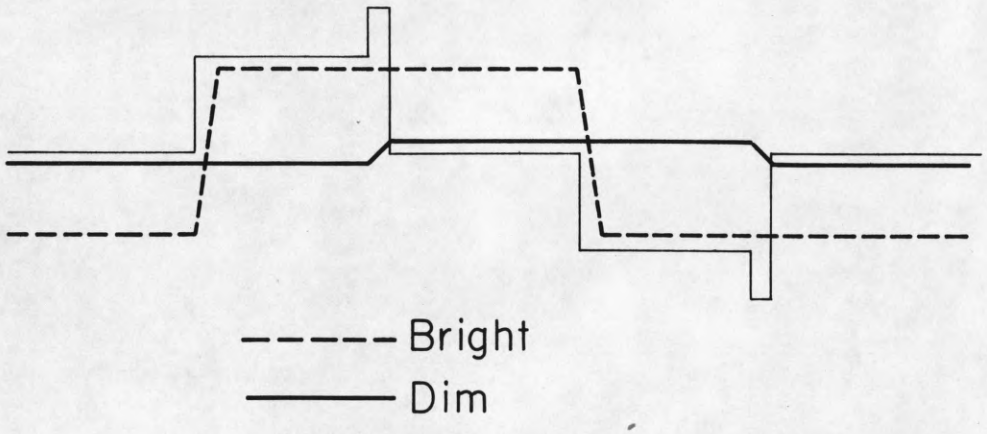

CS-396

Figure 3.18
Representation of Wall Voltages Associated
with Two States of Figure 3.17

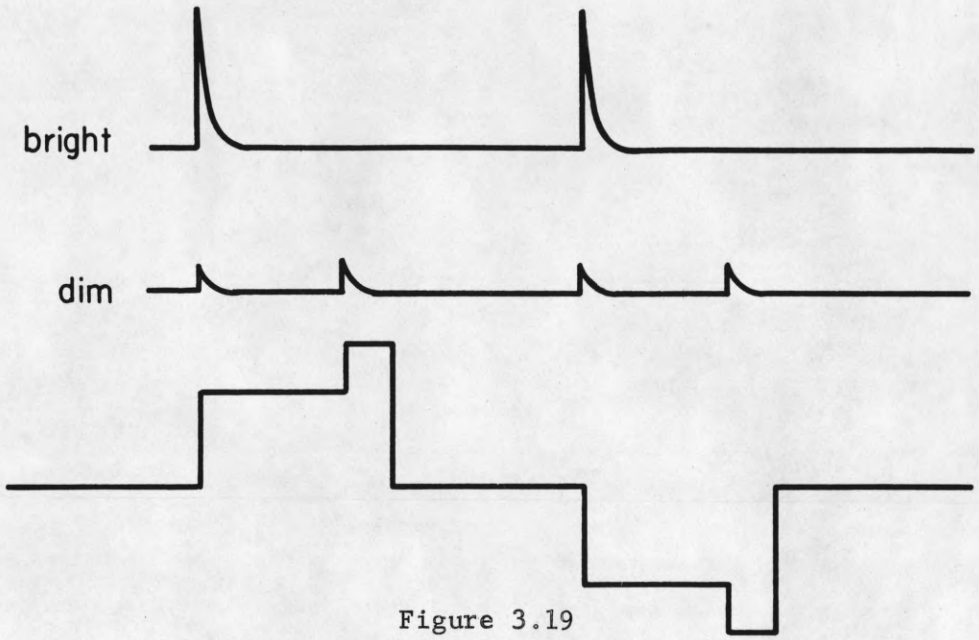

Figure 3.19
Light Output of Two States with a Stepped
Wave Form Sustaining Signal (second mode)

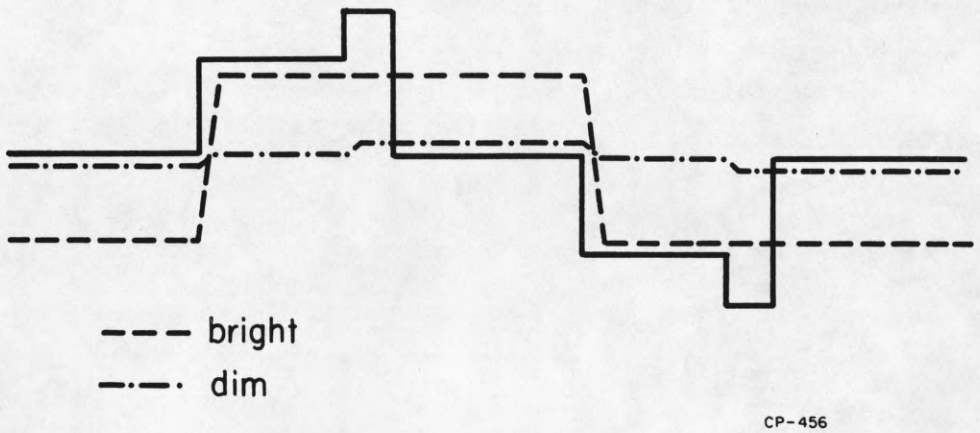

Figure 3.20
Representation of Wall Voltages Associated
with Two States of Figure 3.19

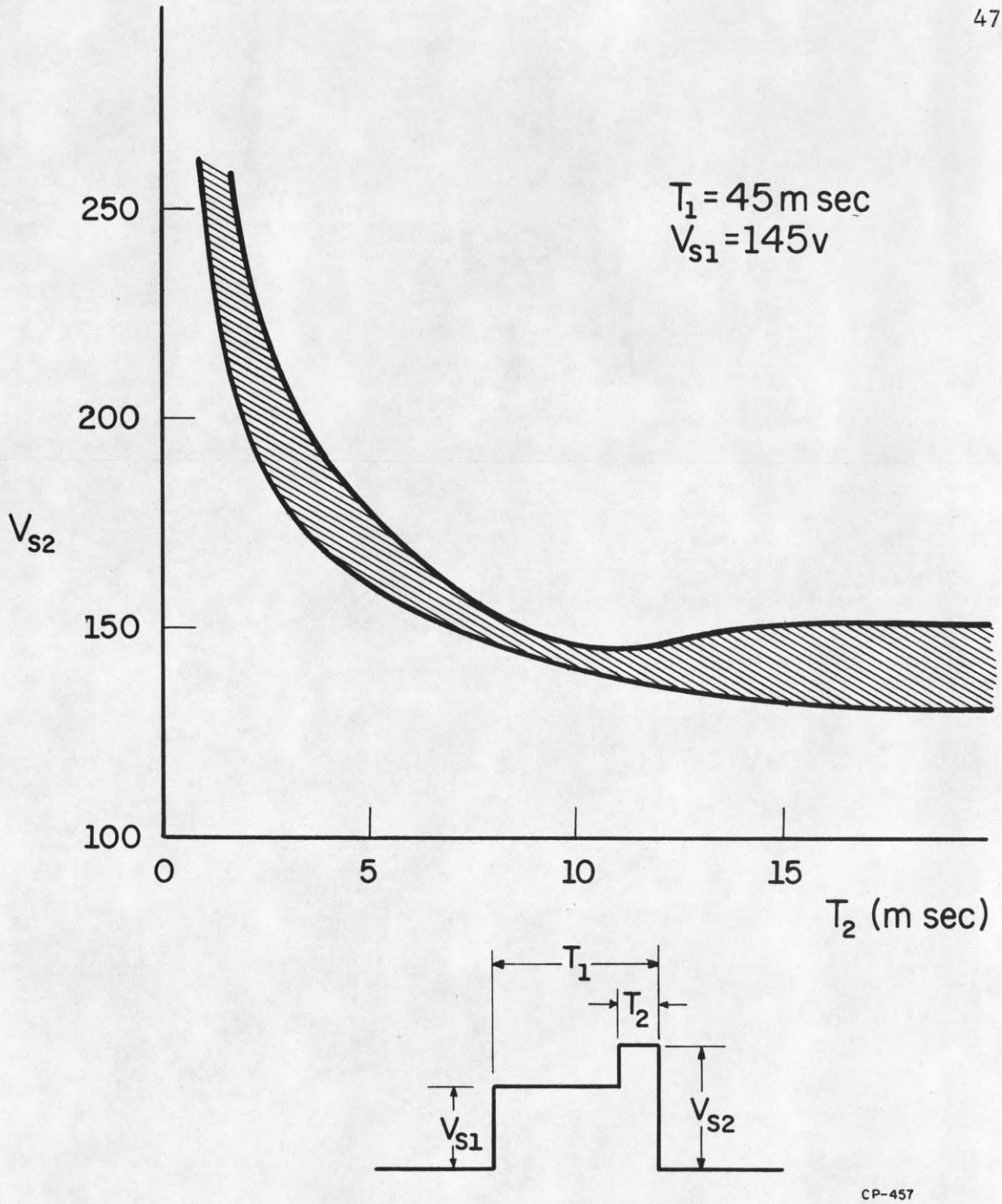

Figure 3.21
Bistable Voltage Range for a Stepped Wave Form
Sustaining Signal (first and second modes)
as a Function of the Width of the Narrow Pulse

CHAPTER 4.

Practical Considerations in Achieving Gray Scale

In order to be of practical use as a panel display the mere possibility of multiple stable states in a single cell is not sufficient. It must be demonstrated that the states can exist in proximity to each other in the panel without unduly influencing the behavior of adjacent cells. The mutli-stable range, i.e., that range of voltage within which all of the cells in a panel can exist in any of the desired states, must be sufficiently large so that panel aging and applied voltage perturbations do not seriously alter the ability of a cell to remain in its selected state. Finally, it must be demonstrated that addressing is possible; that any selected cell in an array may be changed from any one state to any other state without affecting any other cells in the array.

4.1 Spatial Stability

In chapter three it was mentioned that three stable states were achieved with a square wave sustaining signal, however the "off" state could not exist in proximity to the other states because of the particles in the space which would change the characteristics of the "off" cell sufficiently to pull it into one of the other states. Such a system is clearly of little or no use as a three state display. All other methods of achieving multiple stable states examined were spatially stable within a fixed range of sustaining voltages. Ability to exist

in a chosen state in proximity to other states, then, has not shown itself to be a problem except in the special situation described above which must then be eliminated from any practical consideration. Figure 4.1 shows this ability for both a two level rectangular wave in three states and a step wave form in two states.

4.2 Multistable Voltage Range

The multistable voltage range poses perhaps the most significant problem to realization of a multi-level display. In the normal bistable operation of the plasma panel the bistable range is typically thirty volts. With three states the voltage drops to about five volts (see figure 4.2). While this is acceptable for experimentation and has resulted in tri-level displays with excellent stability, it must be remembered that these experiments were conducted on an area of only about one tenth the entire panel and it is reasonable to assume that the voltage range would be even narrower if the whole panel were used. This would result in the necessity of incorporating a high degree of regulation of the voltages used. It is not believed that this is a real deterrent to achieving multiple state panels but merely that it can pose a problem and further work should be done to eliminate it.

4.3 Panel Addressing in Three States

Perhaps the most critical problem to be faced in determining the practicality of gray scale is that of achieving unambiguous yet reliable addresssing techniques for the plasma panel. While an optimization was not considered a part of this research it was felt that the capability

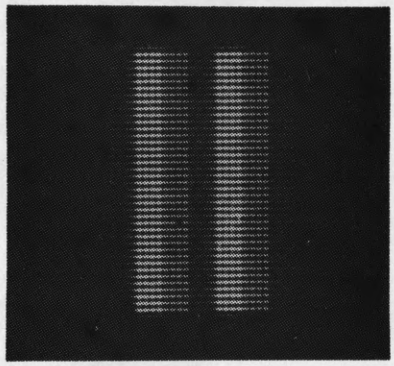

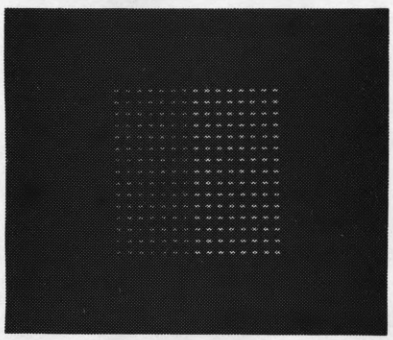

Figure 4.1
Spatial Stability of Multiple States

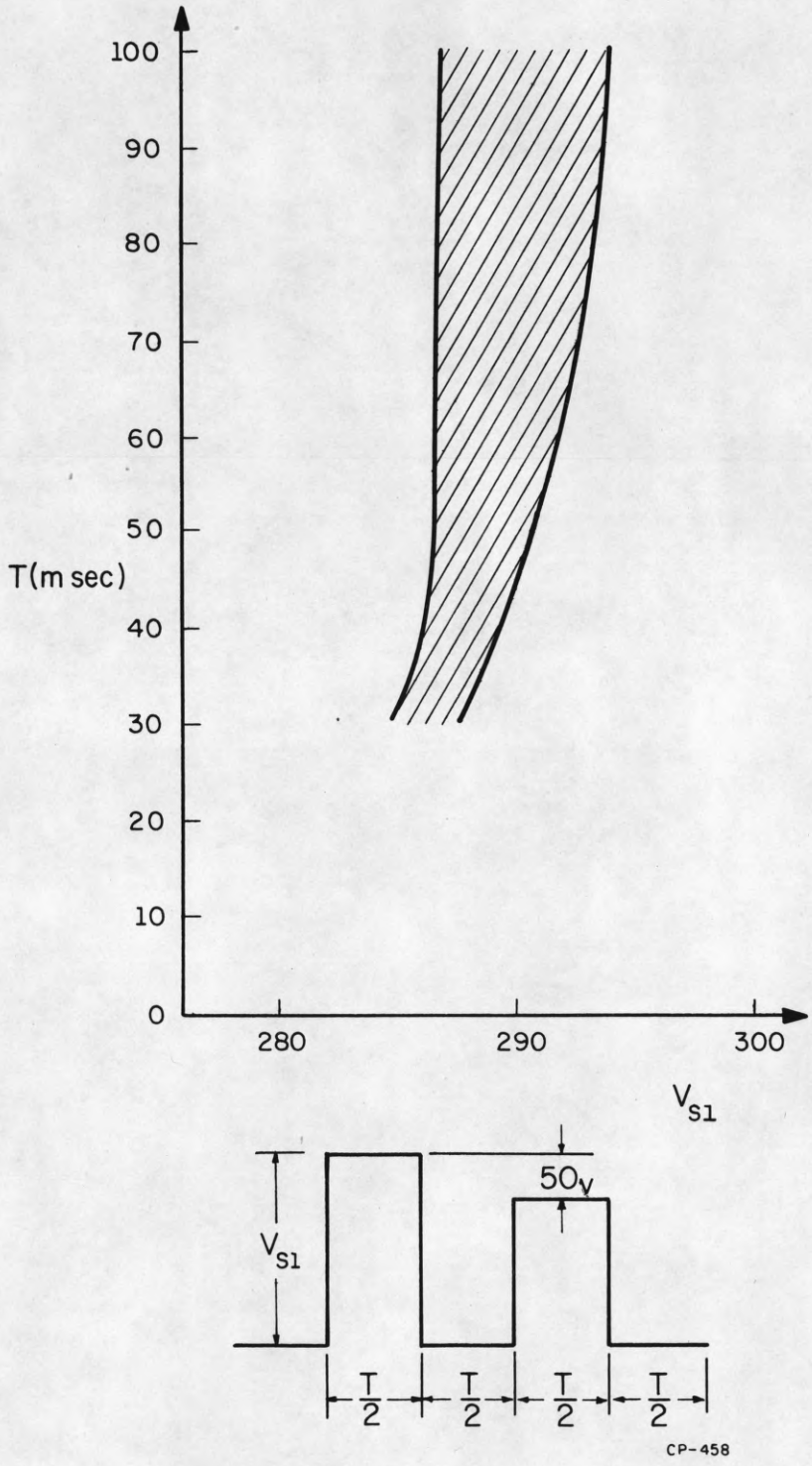

Figure 4.2
Tristable Voltage Range for a Two Level
Square Wave Sustaining Signal

of addressing must be proved in order to make all previous results meaningful. The results below, then should not be considered as the best possible or even particularly recommended, but merely present one method in which addressing can be achieved.

In order to completely address the panel with three states a total of six transitions are possible: Bright-to-medium, bright-to-dim, medium-to-bright, medium-to-dim, dim-to-bright, dim-to-medium. However, because the external circuits do not have information concerning the state of any given cell, successful addressing relies on only three different state transitions, performed in a two stage operation. The first step is the transfer of the cell from its current state to a common address level. The second step is the change of the cell to its desired final state. Thus, if the common level is "medium", bright-to-dim can be the result of the two step process, bright-to-medium and medium-to-dim. If three transitions are demonstrated, into and out of each state, all six transitions are possible. The transitions, bright-to-medium, medium-to-dim, and dim-to-bright, have been achieved. The locations of these transitions on the wall charge curve are shown in figure 4.3.

The achievement of a bright-to-medium transition is accomplished by applying a signal as shown in figure 4.4 on the "X" and "Y" axis of intersection of the desired cell. The resultant voltage across the cell (figure 4.5) is large enough to create a discharge resulting in the transfer of sufficient wall charge to change the state of the cell

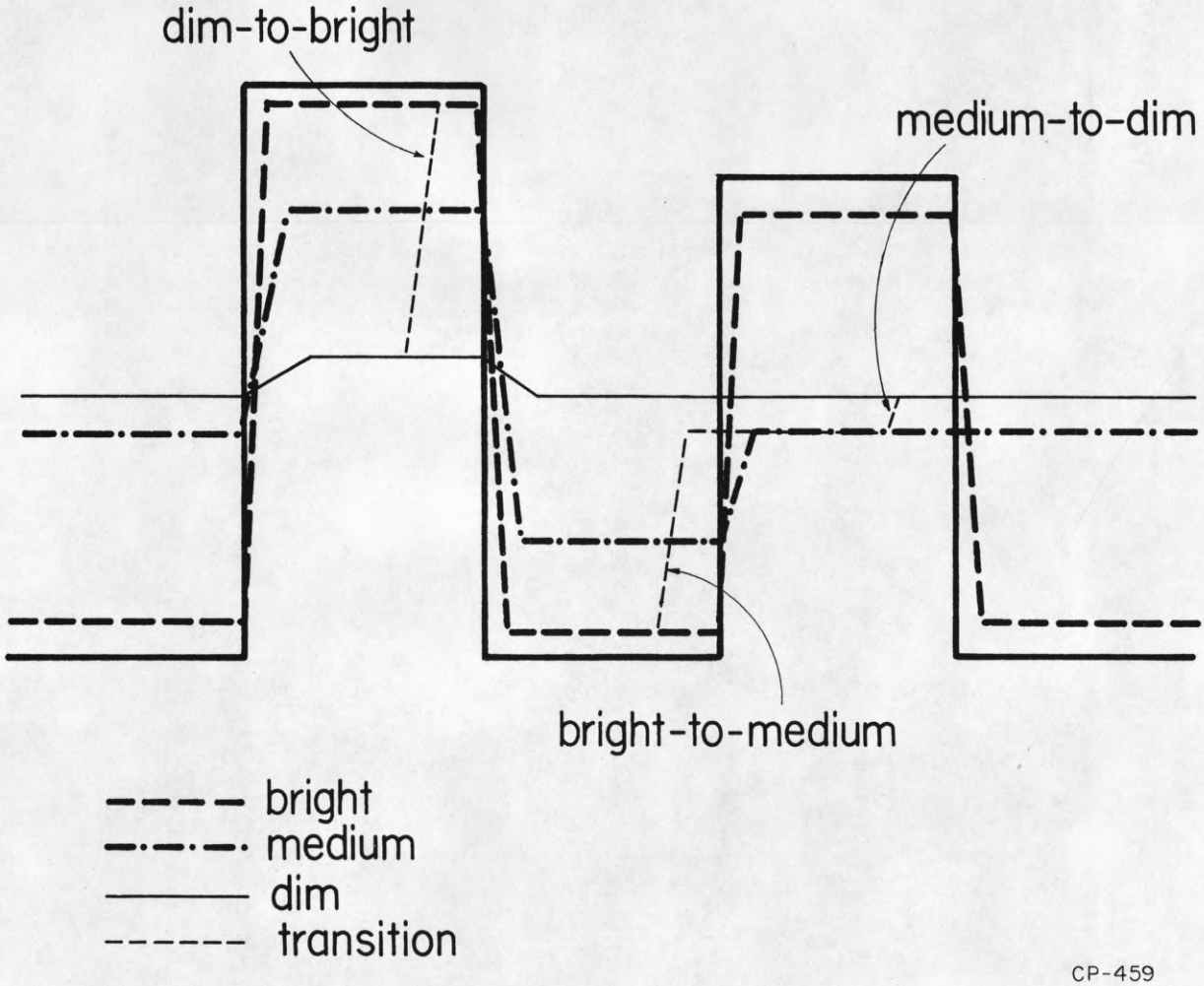

Figure 4.3
Wall Voltage Transition for Three States

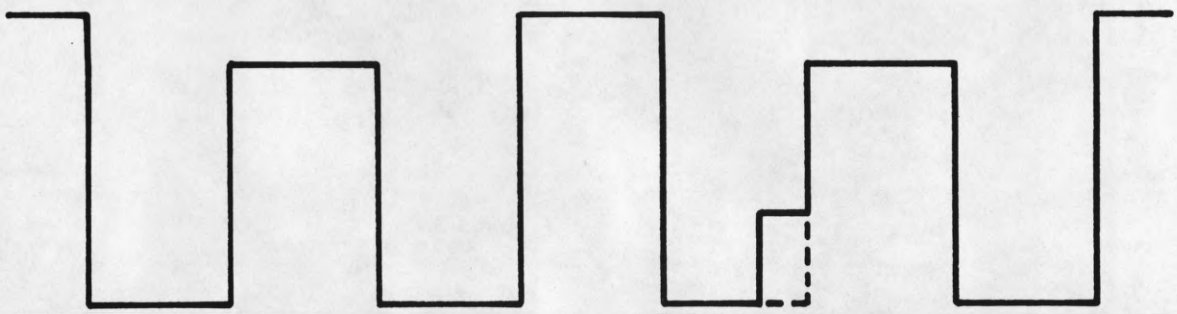

Signal applied to "X" axis

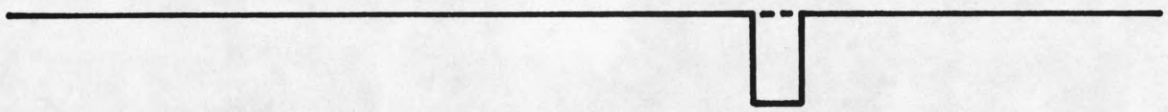

Signal applied to "Y" axis

—— Selected line

---- All other lines

CP-475

Figure 4.4
Applied Wave Forms to Achieve Bright-to-Medium Transition

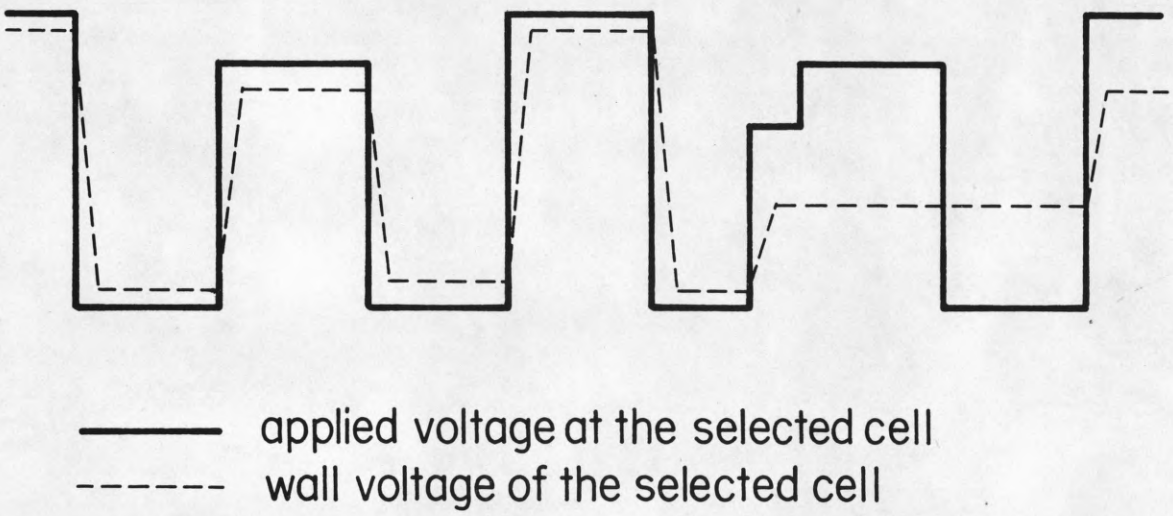

Figure 4.5
Applied Cell Voltage to Achieve Bright-to-Medium Transition

as indicated in figure 4.3. However, the voltage applied to each line, "X" and "Y", is insufficient alone to cause any discharge activity.

A medium-to-dim transition is achieved by applying the signals of figure 4.6 to the two desired axes. The resulting voltage at the addressed cell is shown in figure 4.7.

In order to change the state of a cell from dim-to-bright, adjustment of the sustaining wave form is necessary to prevent half-select problems from occuring on the lines "X" and "Y" from the dim into the medium state. The wave forms of figure 4.8 accomplish both the required state change while providing protection against half-selection. The resultant wave form at the cell is shown in figure 4.9.

Other transitions have been accomplished (e.g., dim-to-medium, medium-to-bright, and bright-to-medium) however, the ones described are sufficient to justify the assertion that reliable addressing in three states is possible with the plasma display panel.

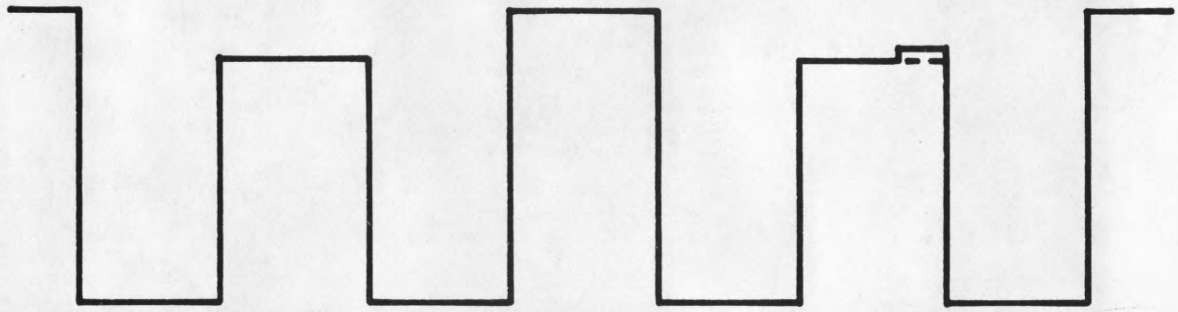

Signal applied to "X" axis

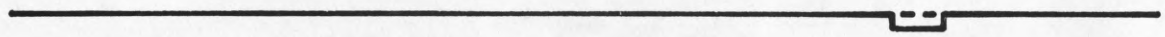

Signal applied to "Y" axis

——— Selected line

----- All other lines

CP-477

Figure 4.6
Applied Wave Forms to Achieve Medium-to-Dim Transition

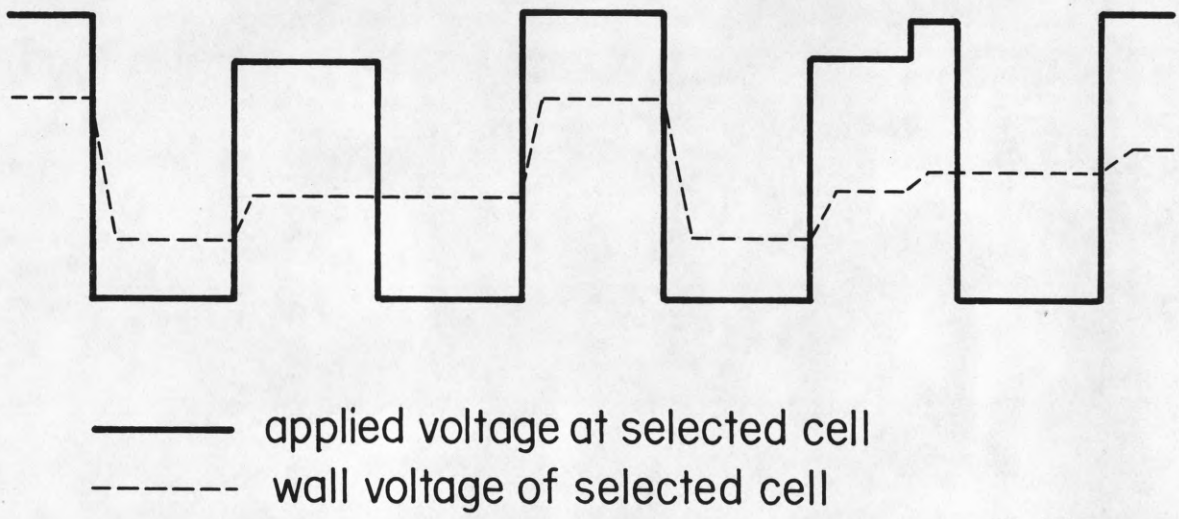

Figure 4.7
Applied Cell Voltage to Achieve Medium-to-Dim Transition

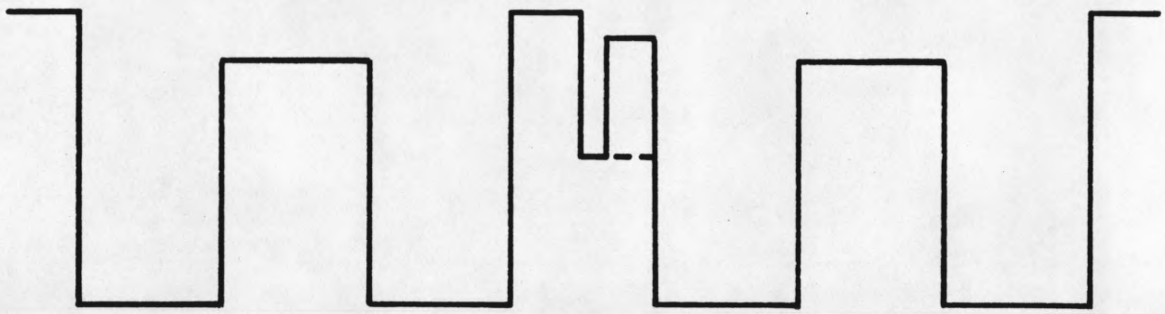

Signal applied to "X" axis

Signal applied to "Y" axis

—— Selected line

---- All other lines

CP-441

Figure 4.8
Applied Wave Forms to Achieve Dim-to-Bright Transition

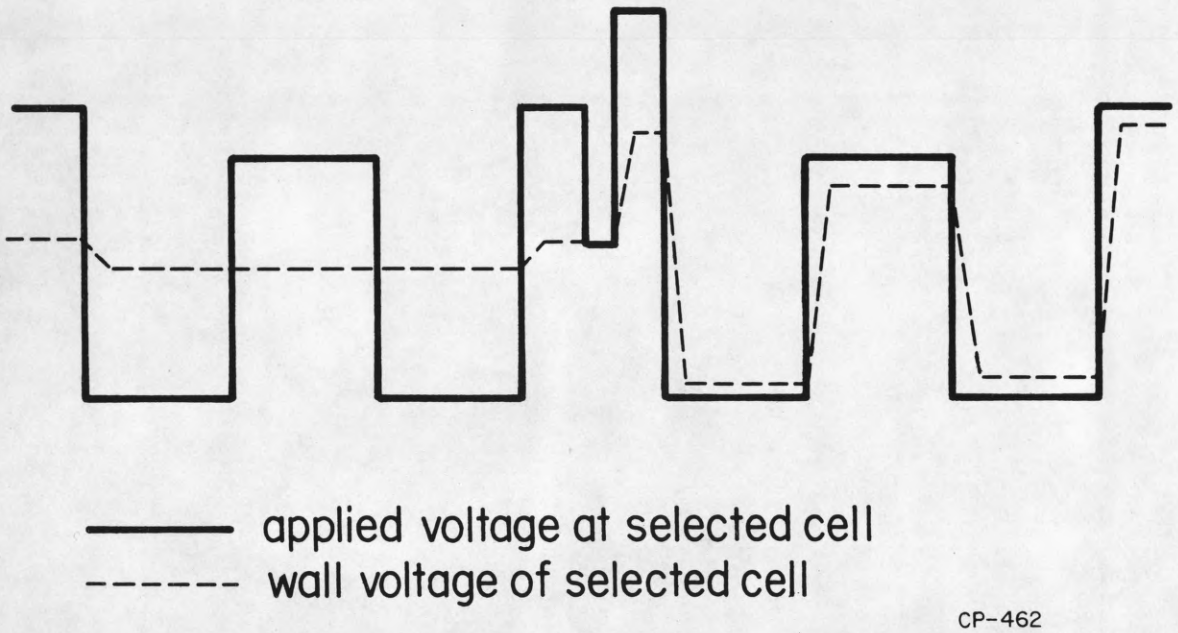

Figure 4.9
Applied Cell Voltage to Achieve Dim-to-Bright Transition

CHAPTER 5.

Conclusions

5.1 Summary of Results

The research described in this report has shown that a plasma display cell exist in several distinct stable firing modes. Additionally, an extended theory upon which a determination of these modes can be based has been derived and tested. The feasibility of maintaining the cells in an array in different stable states, and the realization of an unambiguous cell addressing has been demonstrated.

The uses to which the plasma display panel can be put will be increased significantly with the introduction of even a limited gray scale as demonstrated in this research. In addition to straightforward alpha-numeric and graphical displays as presently envisioned, a three level gray scale will allow for multifunction graphing, limited shading of diagrams and pictorial representations and even ternary memories for computers. This list of possible applications is representative rather than exhaustive and with the development of more levels of gray using the techniques described herein the uses should broaden even further, with reasonable halftone presentation and a full decimal memory as possibilities.

5.2 Suggestions for Further Research

Further research is needed in this area if the full possibilities of multiple stable states are to be realized. Specifically the following

areas need extensive investigation.

The functional relationship among the various parameters associated with the discharge in a plasma cell needs to be quantitatively determined in order to apply the stability criteria to the design of wave forms capable of maintaining several stable states.

The influence of panel parameters (e.g., gas composition, panel and cell construction) upon the discharge must be investigated in order to optimize panel design and achieve a maximum multistable range and level of gray scale.

Panel use studies should consider the application of multiple state technology to determine the feasibility of incorporating gray scale capabilities in system design.

BIBLIOGRAPHY

Arora, B. M., D. L. Bitzer, H. G. Slottow, R. H. Wilson, "The Plasma Display Panel: A New Device for Information Display and Storage," Paper presented at the Eighth National Symposium for Information Display, May, 1967.

Bitzer, D. L., H. G. Slottow, "The Plasma Display Panel - A Digitally Addressable Display with Inherent Memory," Proc. of the Fall Joint Computer Conference, November, 1966.

Bitzer, D. L., H. G. Slottow, et al., "Plasma Display," University of Illinois, Coordinated Science Laboratory Progress Report for March through August, 1968, September, 1968.

Bitzer, D. L., H. G. Slottow, et al., "Plasma Display," University of Illinois, Coordinated Science Laboratory Progress Report for September through June, 1969, August 1969.

Johnson, R. L., "The Application of the Plasma Display Technique to Computer Memory Systems," University of Illinois, Coordinated Science Laboratory Report R-461, April, 1970.

Willson, R. H., "A Capacitively Coupled Bistable Gas Discharge Cell for Computer Controlled Displays," University of Illinois, Coordinated Science Laboratory Report R-303, June, 1966.

APPENDIX A

The Measurement of Charge Transfer Characteristics

Throughout this report numerous references have been made to the charge transfer characteristic. This appendix describes one method of measuring the necessary data upon which to base such a characteristic.

A discharge in a plasma display cell produces a wall charge which is a function of the nature of the discharge and the conditions of the cell prior to the discharge according to the following equation.

$$\Delta V_W = f(V_C, T_1, Q, D, N)$$

where V_C = cell voltage at the time of discharge

T_1 = width of the discharge producing pulse

Q = the polarity of the cell voltage with respect to the wall charge distribution

D = nature of the wall charge distribution prior to discharge

N = nature of the space charge distribution prior to discharge

In order to measure the wall voltage a standard reference is necessary. To obtain this standard, techniques are used to either minimize the effects of the above parameters or hold them constant.

The standard functional relationship is derived by applying the wave form of figure A.1 to the plasma panel, insuring that the square wave sequence is sufficiently long to establish equilibrium. A functional value of the wall voltage is determined by applying a pulse "A" at time "τ" after the

termination of the square wave sequence (figure A.2). "τ" should be about twenty microseconds in order to reduce the space charges to effectively zero, while maintaining the metastable population at approximately its value immediately after the previous discharge.

V_A is adjusted to produce a discharge with magnitude sufficiently large to insure that the cell voltage is much greater than the firing voltage. This precaution eliminates the dependence of the discharge upon any space charges which might otherwise influence the test results. The magnitude of the discharge is measured by recording the light output of the discharge which is assumed to be proportional to the discharge current. From this

$$\Delta V_{WA} = f(V_C, T_1, Q, D, N)$$
$$= f(V_A - V_{W1}, T_1, Q, D, N)$$

The value of V_{W1} is found by adjusting the magnitude of "A" to V_A" such that discharge activity is just present. Then

$$V_A'' - V_{W1} = V_F$$

in which V_F is the minimum magnitude of sustaining signal which will sustain a stable "on" discharge sequence. So that

$$V_{W1} = V_A'' - V_F$$

With this standard relationship established, a second test pulse, "B", is then inserted after the square wave sequence, with the pulse "A" being

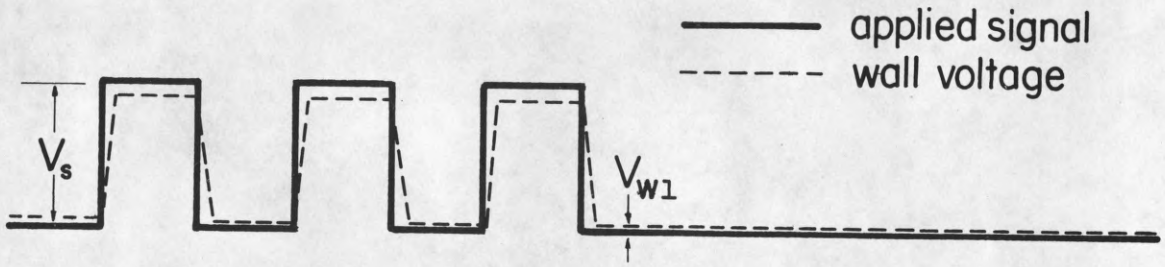

Figure A.1
A Sustaining Wave Form Used in Determining
Charge Transfer Characteristic

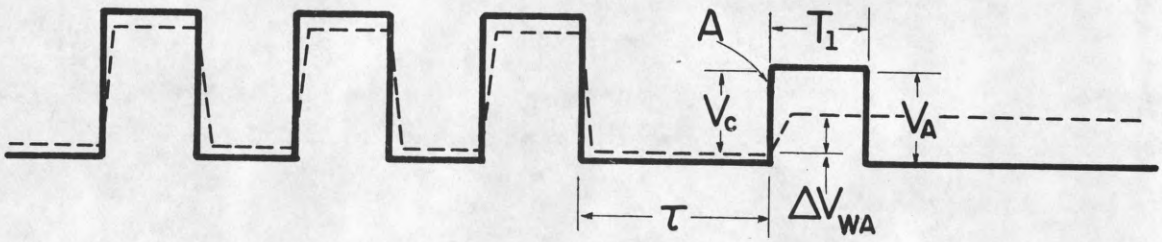

Figure A.2
Determining a Standard Functional Wall Voltage Characteristic

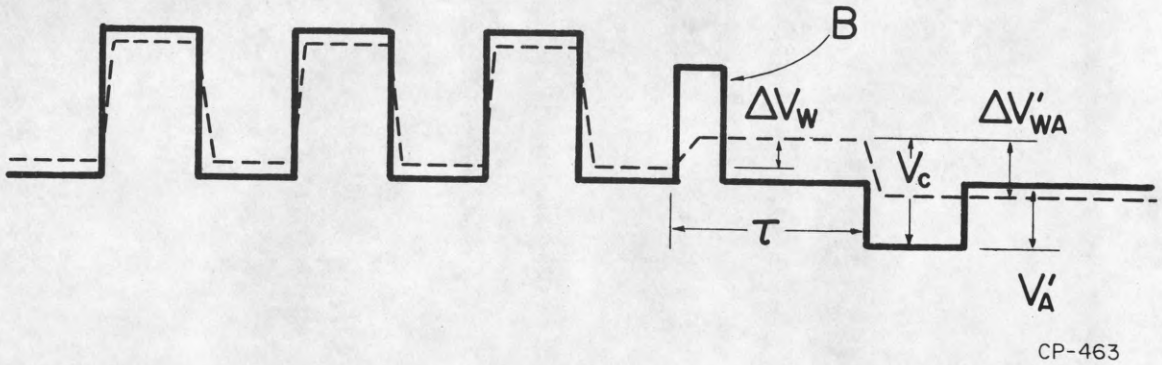

Figure A.3
Wave Form for Determining Charge Transfer Characteristic

moved so that it is now "τ" after the leading edge of the test pulse "B" (figure A.3). This holds "N" a constant. The polarity of pulse "A" is reversed so that Q will remain the same, and because the primary influence of the wall charge distribution results from its maximum and minimum values produced by the preceding discharge, D will be held reasonably constant. The amplitude of "A" is adjusted to $V_{A'}$ such that the discharge produced is the same as the standard. Thus

$$\Delta V_{WA'} = f(V_C, T_1, Q, D, N)$$
$$= f(V_{A'} + \Delta V_W + V_{W1}, T_1, Q, D, N)$$

And because the discharges are the same

$$\Delta V_{WA} = \Delta V_{WA'}$$

or

$$V_{A'} + \Delta V_W + V_{W1} = V_A - V_{W1}$$

$$\Delta V_W = V_A - V_{A'} - 2V_{W1}$$

where ΔV_W may now be plotted as a function of its desired parameters. Figure A.4 illustrates the parameters used in this report.

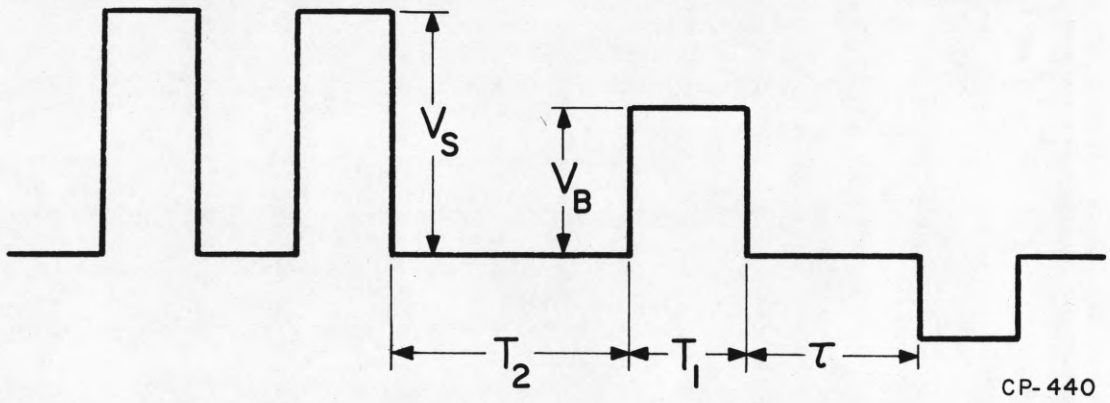

Figure A.4
Illustration of Parameters Influencing
Charge Transfer Characteristic

APPENDIX B

Circuits Used in Achieving Multiple Steady States

A circuit whose block diagram is shown in figure B.1 was used throughout these experiments. The astable multivibrator generated the basic pulses at frequencies from $1KH_z$ to $1MH_z$. The output of this circuit forms the input to a monostable multivibrator which determined the basic pulse width. The frequency divider network was used to provide the inputs for actual signal generation. Signal component generation was provided by twelve logic gates which had the capability of combinational addition of up to eight inputs. The gate outputs formed the inputs to monostable multivibrators which then provided the signals to the drive circuits. Generally the panel was driven in a single-sided mode (figure B.2) but the capability existed to drive it two-sided (figure B.3). Addressing was accomplished using this basic driver with the panel connections modified as in figure B.4.

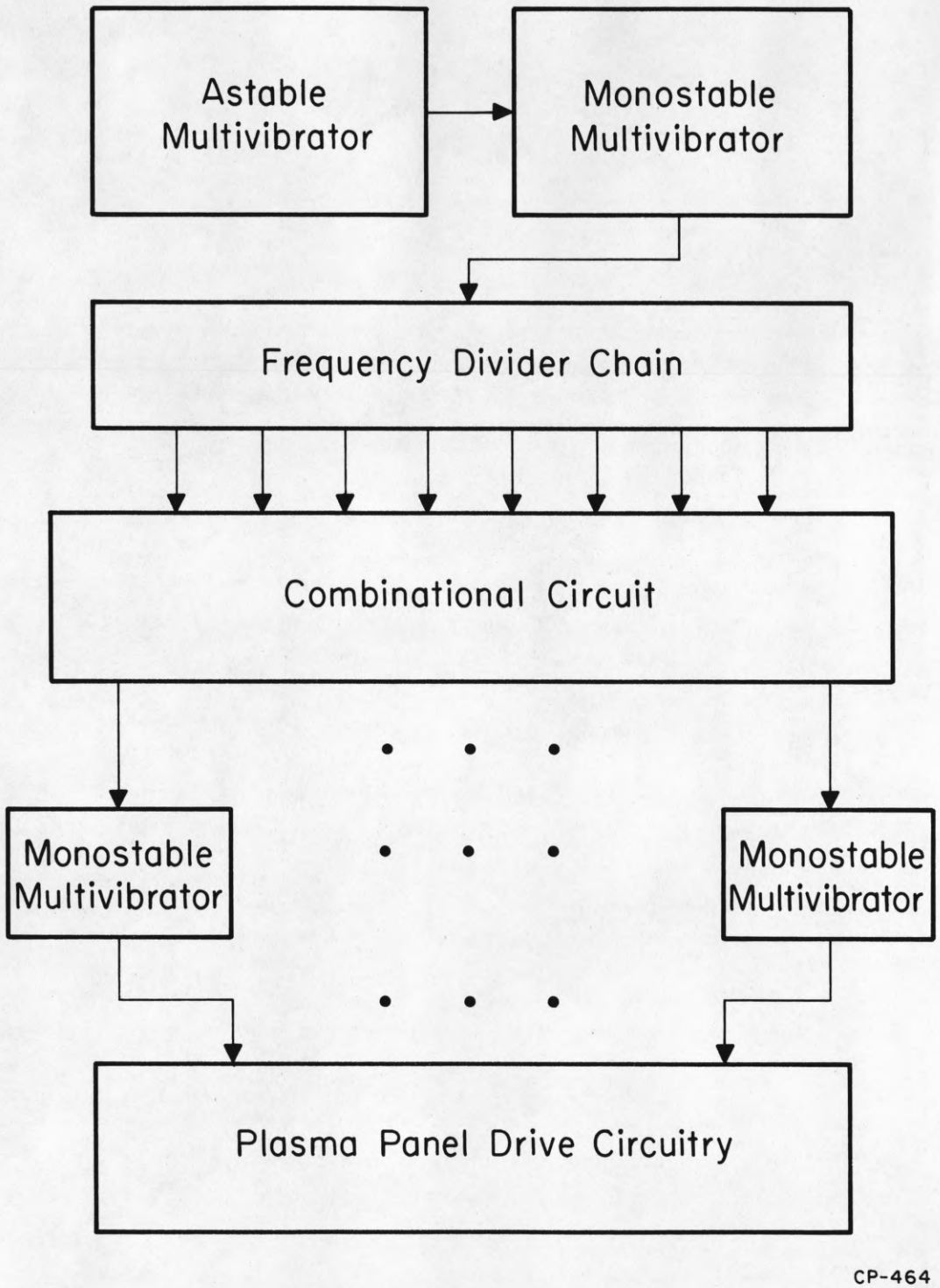

Figure B.1
Block Diagram of Plasma Panel Driving Circuit

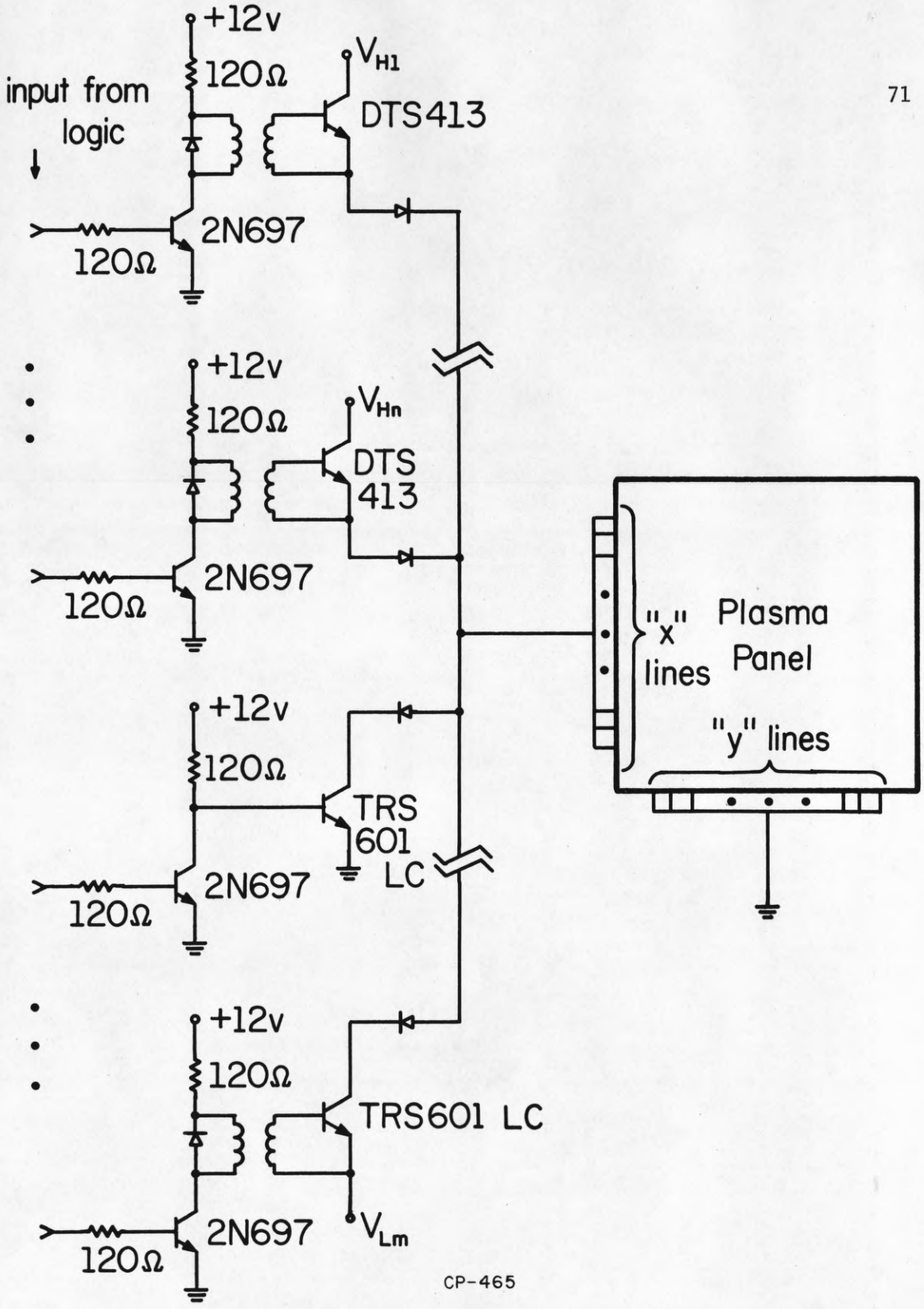

Figure B.2
Single-sided Plasma Panel Driving Circuit

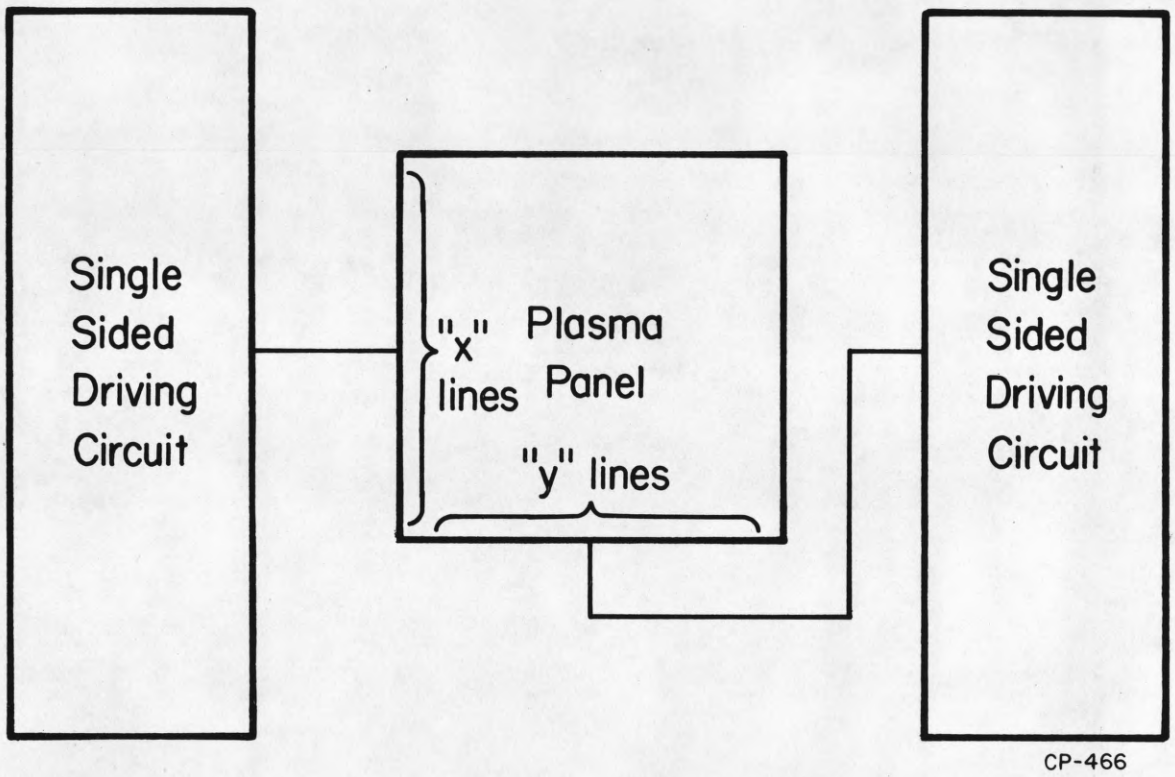

Figure B.3
Two-sided Plasma Panel Driving Circuit

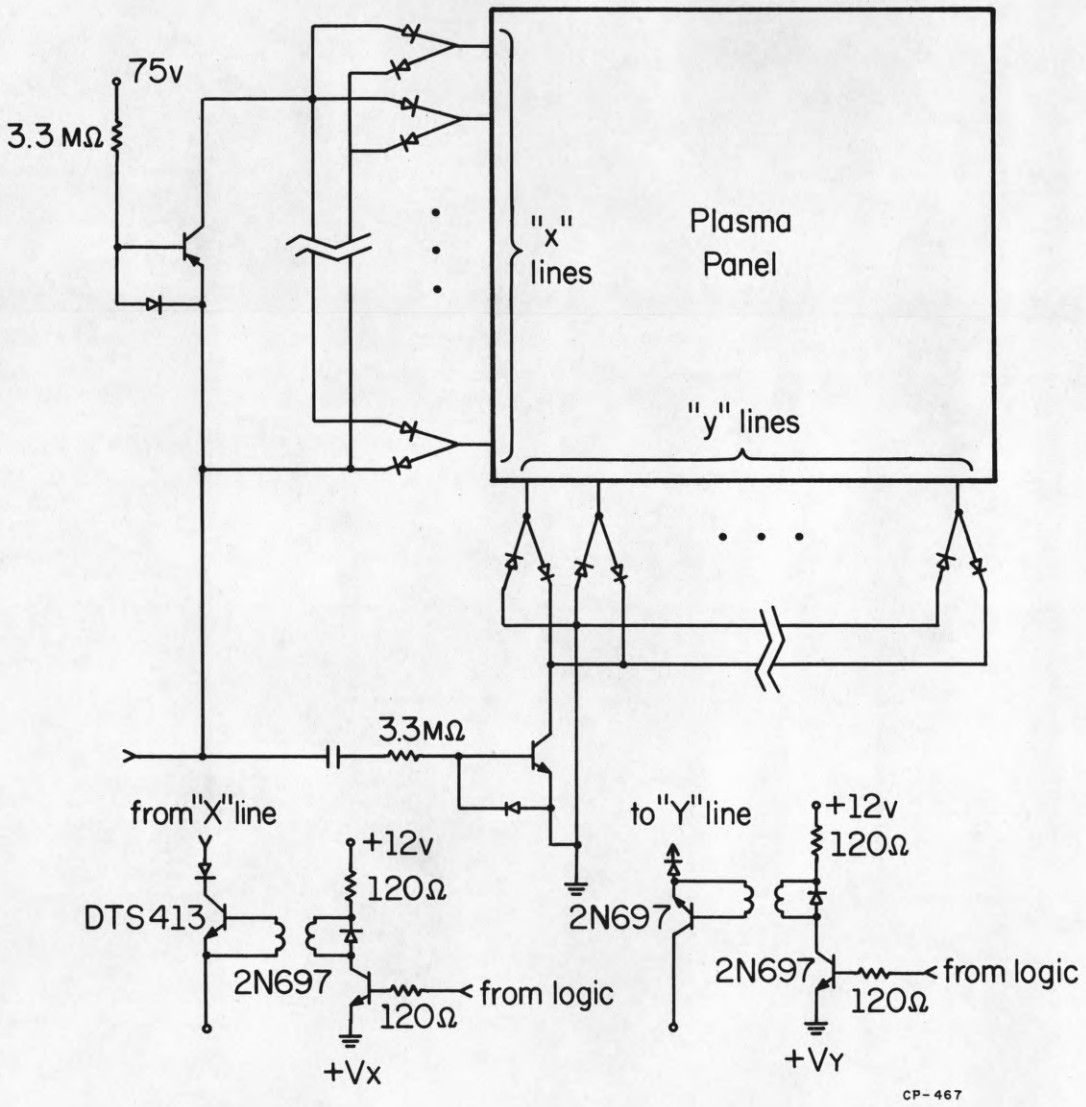

Figure B.4
Plasma Panel Addressing Circuit

VITA

William Dooley Petty was born in Guthrie, Oklahoma, on June 24, 1940, and graduated from Guthrie High School in 1958. He received the B.S. degree from the United States Military Academy in 1962. After four years of military service with the Corps of Engineers, Mr. Petty entered the University of Illinois in 1966. He received the M.S. degree in 1968 and his Ph.D. in Electrical Engineering from that institution in 1970.

Mr. Petty was an instructor at the United States Army School, Europe during his last two years of military service, and he has taught courses in circuits and electronics for the past four years at the University of Illinois. He currently holds the academic rank of instructor. From 1967 to the present, Mr. Petty has worked at the Coordinated Science Laboratory of the University of Illinois in the area of Plasma Display research.

Distribution List as of 1 November 1970

ESD (ESTI)
L. G. Hanscom Field
Bedford, Mass. 01731 2 copies

Naval Air Systems Command
AIR 03
Washington, D. C. 20360 2 copies

Commanding General
U.S. Army Electronics Command
Fort Monmouth, New Jersey 07703
Attn: AMSEL-RD-PB (2 copies)
(Miss F. Morris)

Naval Electronic Systems Command
ELEX 03, Room 2046 Munitions Building
Department of the Navy
Washington, D. C. 20360 2 copies

Director
Naval Research Laboratory
Washington, D. C. 20390
Washinton, D. C. 2027 6 copies

Commander
U.S. Naval Ordnance Laboratory
Attn: Librarian
White Oak, Md. 20910 2 copies

Dr. L. A. Wood, Director
Electronic and Solid State Sciences
Air Force Office of Scientific Research
1400 Wilson Boulevard
Arlington, Virginia 22209 5 copies

Director, Electronic Programs
Attn: Code 427
Office of Naval Research
800 North Quincy Street
Arlington, Virginia 22217 3 copies

Defense Documentation Center
Attn: DDC-TCA
Cameron Station
Alexandria, Virginia 222314 50 copies

Commanding General
Attn: STEWS-RE-L, Technical Library
White Sands Missile Range
New Mexico 88002 (2 copies)

Commander
Naval Electronics Laboratory Center
Attn: Library
San Diego, Calif. 92152 2 copies

Dr. L. M. Hollingsworth
AFCRL (CRN)
L. G. Hanscom Field
Bedford, Massachusetts 01731

Division of Engineering and Applied Physics
210 Pierce Hall
Harvard University
Cambridge, Massachusetts 02138

Director
Research Laboratory of Electronics
Massachusetts Institute of Technology
Cambridge, Massachusetts 02139

Miss R. Joyce Harman
Project MAC, Room 810
545 Technology Square
Cambridge, Mass. 02139

Professor R. H. Rediker
Electrical Engineering, Prof.
Mass. Institute of Technology
Building 13-3050
Cambridge, Mass. 02139

Raytheon Company
Research Division Library
28 Seyon Street
Waltham, Massachusetts 02154

Sylvania Electronic Systems
Applied Research Laboratory
Attn: Documents Librarian
40 Sylvan Road
Waltham, Mass. 02154

Commanding Officer
Army Materials & Mechanics Res. Center
Attn: Dr. H. Priest
Watertown Arsenal
Watertown, Massachusetts 02172

MIT Lincoln Laboratory
Attn: Library A-082
P.O. Box 73
Lexington, Mass. 02173

Commanding Officer
Office of Naval Research Branch Office
495 Summer Street
Boston, Massachusetts 02210

Commanding Officer (Code 2064)
U.S. Naval Underwater Sound Laboratory
Fort Trumbull
New London, Connecticut 06320

Dept. of Eng. & Applied Science
Yale University
New Haven, Conn. 06520

Commanding General
U.S. Army Electronics Command
Attn: AMSEL-CT-A
Fort Monmouth, New Jersey 07703

Commanding General
U.S. Army Electronics Command
Attn: AMSEL-CT-D
Fort Monmouth, New Jersey 07703

Commanding General
U.S. Army Electronics Command
Attn: AMSEL-CT-I
Fort Monmouth, New Jersey 07703

Commanding General
U.S. Army Electronics Command
Attn: AMSEL-CT-L (Dr. W. S. McAfee)
Fort Monmouth, New Jersey 07703

Commanding General
U.S. Army Electronics Command
Attn: AMSEL-CT-O
Fort Monmouth, New Jersey 07703

Commanding General
U.S. Army Electronics Command
Attn: AMSEL-CT-R
Fort Monmouth, New Jersey 07703

Commanding General
U.S. Army Electronics Command
Fort Monmouth, New Jersey 07703
Attn: AMSEL-CT-S

Commanding General
U.S. Army Electronics Command
Attn: AMSEL-DL
Fort Monmouth, New Jersey 07703

Commanding General
U.S. Army Electronics Command
Attn: AMSEL-CC-DD
Fort Monmouth, N. J. 07703

Commanding General
U.S. Army Electronics Command
Attn: AMSEL-KL-D
Fort Monmouth, New Jersey 07703

Commanding General
U.S. Army Electronics Command
Attn: AMSEL-KL-E
Fort Monmouth, New Jersey 07703

Commanding General
U.S. Army Electronics Command
Attn: AMSEL-KL-I
Fort Monmouth, New Jersey 07703

Commanding General
U.S. Army Electronics Command
Attn: AMSEL-KL-SM
Fort Monmouth, New Jersey 07703

Commanding General
U.S. Army Electronics Command
Attn: AMSEL-KL-SM
Fort Monmouth, New Jersey 07703

Commanding General
U.S. Army Electronics Command
Attn: AMSEL-KL-S
Fort Monmouth, New Jersey 07703

Commanding General
U.S. Army Electronics Command
Attn: AMSEL-KL-T
Fort Monmouth, New Jersey 07703

Commanding General
U.S. Army Electronics Command
Attn: AMSEL-NL-A
Fort Monmouth, New Jersey 07703

Commanding General
U.S. Army Electronics Command
Attn: AMSEL-NL-C
Fort Monmouth, New Jersey 07703

Commanding General
U.S. Army Electronics Command
Attn: AMSEL-NL-D (Dr. H. Bennett)
Fort Monmouth, New Jersey 07703

Commanding General
U.S. Army Electronics Command
Attn: AMSEL-NL-P
Fort Monmouth, New Jersey 07703

Commanding General
U.S. Army Electronics Command
Attn: AMSEL-SC
Fort Monmouth, New Jersey 07703

Commanding General
U.S. Army Electronics Command
Attn: AMSEL-VL-D
Fort Monmouth, New Jersey 07703

Commanding General
U.S. Army Electronics Command
Attn: AMSEL-VL-F
Fort Monmouth, New Jersey 07703

Commanding General
U.S. Army Electronics Command
Attn: AMSEL-WL-D
Fort Monmouth, New Jersey 07703

Commanding General
U.S. Army Electronics Command
Attn: AMSEL-XL-DT
Fort Monmouth, New Jersey 07703

Commanding General
U.S. Army Electronics Command
Attn: AMSEL-XL-D
Fort Monmouth, New Jersey 07703

Mr. Norman J. Field, AMCPM-AA-PM
Program Management Division
Project AACOMS
USAECOM, Bldg-2525
Fort Monmouth, New Jersey 07703

Project Manager
Common Positioning & Navigation Systems
Attn: Harold H. Bahr (AMCPM-NS-TM),
Bldg. 439
U.S. Army Electronics Command
Fort Monmouth, New Jersey 07703

Dr. H. K. Ziegler, Chief Scientist
Army Member TAC/JSEP (AMSEL-SC)
U.S. Army Electronics Command
Fort Monmouth, New Jersey 07703

Mr. I. A. Balton, AMSEL-XL-D
Executive Secretary, TAC/JSEP
U.S. Army Electronics Command
Fort Monmouth, New Jersey 07703

Commanding General
U.S. Army Electronics Command
Attn: AMSEL-XL-G (Dr. S. Kronenberg)
Fort Monmouth, New Jersey 07703

Commanding General
U.S. Army Electronics Command
Attn: AMSEL -XL-H (Dr. R. G. Buser)
Fort Monmouth, New Jersey 07703

U.S. Army Munitions Command
Attn: Science & Technology
Info. Br., Bldg. 59
Picatinny Arsenal, SMUPA-RT-S
Dover, New Jersey 07801

European Office of Aerospace Research
Technical Information Office
Box 14, FPO New York 09510

Director
Columbia Radiation Laboratory
Columbia University
538 West 120th St.
New York, New York 10027

New York University
Engineering Library
Bronx, New York 10453

Mr. Jerome Fox, Research Coordinator
Polytechnic Institute of Brooklyn
333 Jay St.
Brooklyn, New York 11201

Airborne Instruments Labroratory
Deerpark, New York 11729

Dr. W. R. Lepage, Chairman
Syracuse University
Dept. Of Electrical Engineering
Syracuse, New York 13210

Rome Air Development Center
Attn: Documents Library (EMTLD)
Griffiss Air Force Base, New York 13440

Mr. H. E. Webb (EMBIS)
Rome Air Development Center
Griffiss Air Force Base, New York 13440

Professor James A Cadzow
Department of Electrical Engineering
State University of New York at Buffalo
Buffalo, New York 14214

Dr. A. G. Jordan
Head of Dept. of Electrical Engineering
Carnegie-Mellon University
Pittsburgh, Penn. 15213

Hunt Library
Carnegie-Mellon University
Schenley Park
Pittsburgh, Penn.

Lehigh University
Department of Electrical Engineering
Bethelehem, Penn. 18015

Commander (ADL)
Naval Air Development Center
Attn: NADC Library
Johnsville, Warminister, Penn. 18974

Technical Director (SMUFA-A2000-107-1)
Frankford Arsenal
Philadelphia, Penn. 19137

Mr. M. Zane Thornton, Chief, Network
Engineering, Communications and
Operations Branch, Lister Hill
National Center/Biomedical Communications
8600 Rockville Pike
Bethesda, Maryland 20014

U.S. Post Office Department
Library - Room 6012
12th & Pennsylvania Ave. N.W.
Washington, D.C. 20260

Technical Library
DDR&E
Room 3C-122, The Pentagon
Washington, D.C. 20301

Director for Materials Sciences
Advanced Research Projects Agency
Department of Defense
Washington, D.C. 20301

Assistant Director, (Research)
Office of Director of Defense Research
& Engineering
Pentagon, Rm. 3C128
Washington, D.C. 20301

Chief, R & D Division (340)
Defense Communications Agency
Washington, D.C. 20305

Commanding General
U. S. Army Material Command
Attn: AMCRD-TP
Washington, D.C. 20315

Hq. USAF (AFRDD)
The Pentagon
Washington, D.C. 20330

Hq. USAF (AFRDDG)
The Pentagon
Washington, D.C. 20330

Hq. USAF (AFRDSD)
The Pentagon
Washington, D.C. 20330

AFSC (SCTSE)
Andrews Air Force Base, Maryland 20331

Dr. I. R. Mirman
Hq. AFSC (SGGP)
Andrews AFB, Maryland 20331

Naval Ship Systems Command
Ship 031
Washington, D.C. 20360

Naval Ship Systems Command
Ship 035
Washington, D.C. 20360

U.S. Naval Oceanographic Office
Attn: M. Rogofsky, Librarian (Code 640)
Washington, D.C. 20390

Commander
U.S. Naval Security Group Command
Attn: G43
3801 Nebraska Avenue
Washington, D.C. 20390

Director
Naval Research Laboratory
Washington, D.C. 20390
Attn: Dr. A. Brodizinsky, Sup. Elec. Div.

Director
Naval Research Laboratory
Washington, D.C. 20390
Attn: Maury Center Library (Code 8050)

Director
Naval Research Laboratory
Washington, D.C. 20390
Attn: Dr. W. C. Hall, Code 7000

Director
Naval Research Laboratory
Attn: Library, Code 2029 (ONRL)
Washington, D.C. 20390

Dr. G. M. R. Winkler
Director, Time Service Division
U.S. Naval Observatory
Washington, D.C. 20390

Colonel E. P. Gaines, Jr.
ACDA/FO
1901 Pennsylvania Ave. N.W.
Washington, D.C. 20451

Commanding Officer
Harry Diamond Laboratories
Attn: Mr. Berthold Altman (AMXDO-TI)
Connecticut Ave. & Van Ness St., N.W.
Washington, D.C. 20438

Central Intelligence Agency
Attn: CRS/ADD Publications
Washington, D.C. 20505

Dr. H. Harrison, Code RRE
Chief, Electrophysics Branch
National Aeronautics & Space Admin.
Washington, D.C. 20546

The John Hopkins University
Applied Physics Laboratory
Attn: Document Librarian
8621 Georgia Avenue
Silver Spring, Maryland 20910

Commanding Officer (AMXRD-BAT)
U.S. Army Ballistics Research
Laboratory
Aberdeen Proving Ground
Aberdeen, Maryland 21005

Technical Director
U.S. Army Land Warfare Laboratory
Aberdeen Proving Ground
Aberdeen, Maryland 21005

Electromagnetic Compatibility
Analysis Center (ECAC)
Attn: ACOAT
North Severn
Annapolis, Maryland 21402

Commanding Officer
U.S. Army Engineer Topographic Labs
Attn: STINFLO Center
Fort Belvoir, Virginia 22060

Director (NV-D)
Night Vision Laboratory, USAECOM
Fort Belvoir, Va. 22060

U.S. Army Mobility Equipment Research and Development Center
Attn: Technical Document Center, Bldg. 315
Fort Belvoir, Virginia 22060

Dr. Alvin D. Schnitzler
Institute for Defense Analyses
Science and Technology Division
400 Army-Navy Drive
Arlington, Va. 22202

Director
Physical & Engineering Sciences Division
3045 Columbia Pike
Arlington, Va. 22204

Commanding General
U.S. Army Security Agency
Attn: IARD-T
Arlington Hall Station
Arlington, Virginia 22212

Dr. Joel Trimble, Code 437
Information Systems Branch
Office of Naval Research
800 North Quincy Street
Arlington, Virginia 22217

Commanding General
USACDC Institute of Land Combat
Attn: Technical Library, Rm. 636
2461 Eisenhower Avenue
Alexandria, Virginia 22314

Director
USA Advanced Material Concepts Agency
2461 Eisenhower Avenue
Alexandria, Virginia 22314

VELA Seismological Center
300 North Washington St.
Alexandria, Virginia 22314

U.S. Naval Weapons Laboratory
Dahlgren, Virginia 22448

Research Laboratories for the Eng. Sciences, School of Engineering and Applied Science
University of Virginia
Charlottesville, Virginia 22903

Dr. Herman Robl
Deputy Chief Scientist
U.S. Army Research Office (Durham)
Box CM, Duke Station
Durham, North Carolina 27706

Richard O. Ulsh (CRDARD-IP)
U.S. Army Research Office (Durham)
Box CM, Duke Station
Durham, North Carolina 27706

ADTC (ADBPS-12)
Eglin AFB, Florida 32542

Commanding Officer
Naval Training Device Center
Orlando, Florida 32813

Technical Library, AFETR
(ETV,MU-135)
Patrick AFB, Florida 32925

Commanding General
U.S. Army Missile Command
Attn: AMSMI-RR
Redstone Arsenal, Alabama 35809

Redstone Scientific Information Center
Attn: Chief, Document Section
U.S. Army Missile Command
Redstone Arsenal, Alabama 35809

AUL3T-9663
Maxwell AFB, Alabama 36112

Hq. AEDC (AETS)
Attn: Library/Documents
Arnold AFB, Tennessee 37389

Case Institute of Technology
Engineering Division
University Circle
Cleveland, Ohio 44106

NASA Lewis Research Center
Attn: Library
21000 Brookpark Road
Cleveland, Ohio 44135

Director
Air Force Avionics Laboratory
Wright-Patterson AFB, Ohio 45433

AFAL (AVT) Dr. H. V. Noble, Chief
Electronics Technology Division
Air Force Avionics Laboratory
Wright-Patterson AFB, Ohio 45433

Dr. Robert E. Fontana
Head, Dept. of Electrical Engineering
Air Force Institute of Technology
Wright-Patterson AFB, Ohio 45433

AFAL/TEA
Wright-Patterson Air Force Base, Ohio 45433

Department of Electrical Engineering
Clippinger Laboratory
Ohio University
Athens, Ohio 45701

Commanding Officer
Naval Avionics Facility
Indianapolis, Indiana 46241

Dr. John C. Hancock, Head
School of Electrical Engineering
Purdue University
Lafayette, Indiana 47907

Professor Joseph E. Rowe
Chairman, Department of Electrical Engineering
The University of Michigan
Ann Arbor, Michigan 48104

Dr. G. J. Murphy
The Technological Institute
Northwestern University
Evanston, Ill. 60201

Commanding Officer
Office of Naval Research Branch Office
219 South Dearborn St.
Chicago, Illinois 60604

Illinois Institute of Technology
Dept. of Electrical Engineering
Chicago, Illinois 60616

Deputy for Res. and Eng. (AMSE-DRE)
U.S. Army Weapons Command
Rock Island Arsenal
Rock Island, Illinois 61201

Commandant
U.S. Army Command & General Staff College
Attn: Acquisitions, Library Division
Fort Leavenworth, Kansas 66027

Department of Electrical Engineering
Rice University
Houston, Texas 77001

Dr. Billy Welch
USAFSAM (SMC)
Brooks AFB, Texas 78235

HQ AMD (AMR)
Brooks AFB, Texas 78235

USAFSAM (SMKOR)
Brooks AFB, Texas 78235

Mr. B. R. Locke
Technical Adviser, Requirements
USAF Security Service
Kelly Air Force Base, Texas 78241

Director
Electronics Research Center
The University of Texas at Austin
Eng.-Science Bldg. 110
Austin, Texas 78712

Department of Electrical Engineering
Texas Technological University
Lubbock, Texas 79409

Commandant
U.S. Army Air Defense School
Attn: Missile Sciences Div., C&S Dept.
P.O. Box 9390
Fort Bliss, Texas 79916

Director
Aerospace Mechanics Sciences
Frank J. Seiler Research Laboratory (OAR)
USAF Academy
Colorado Springs, Colorado 80840

Director of Faculty Research
Department of the Air Force
U.S. Air Force Academy
Colorado Springs, Colorado 80840

Major Richard J. Gowen
Tenure Associate Professor
Dept. of Electrical Engineering
U.S. Air Force Academy
Colorado Springs, Colorado 80840

Academy Library (DFSLB)
U.S. Air Force Academy
Colorado Springs, Colorado 80840

M. A. Rothenberg (STEPD-SC(S))
Scientific Director
Desert Test Center
Bldg. 100, Soldiers' Circle
Fort Douglas, Utah 84113

Utah State University
Dept. of Electrical Engineering
Logan, Utah 84321

School of Engineering Sciences
Arizona State University
Tempe, Arizona 85281

Commanding General
U.S. Army Strategic Communications Command
Attn: SCC-CG-SAE
Fort Huachuca, Arizona 85613

The University of Arizona
Dept. of Electrical Engineering
Tucson, Arizona 85721

Capt. C. E. Baum
AFWL (WLRE)
Kirkland AFB, New Mexico 87117

Los Alamos Scientific Laboratory
Attn: Report Library
P.O. Box 1663
Los Alamos, New Mexico 87544

Commanding Officer
Atmospheric Sciences Laboratory
White Sands Missile Range, N.M. 88002

Commanding Officer
(AMSEL-BL-WS-R)
Atmospheric Sciences Laboratory
White Sands Missile Range,
New Mexico 88002

Chief, Missile Electronic Warfare
Tech. Area
(AMSEL-WL-M)
Electronic Warfare Laboratory, USAFCOM
White Sands Missile Range, N.M. 88002

Director
Electronic Sciences Lab.
University of Southern California
Los Angeles, Calif. 90007

Engineering & Mathematical Sciences
Library
University of California at Los Angeles
405 Hilgred Avenue
Los Angeles, Calif. 90024

Aerospace Corporation
P.O. Box 95085
Los Angeles, California 90045
Attn: Library Acquisitions Group

HQ SAMSO (SMTTA/Lt. Belate)
AF Unit Post Office
Los Angeles, Calif. 90045

Dr. Sheldon J. Wells
Electronic Properties Information Center
Mail Station E-175
Hughes Aircraft Company
Culver City, California 90230

Director, USAF PROJECT RAND
Via: Air Force Liaison Office
The RAND Corporation
Attn: Library D
1700 Main Street
Santa Monica, Calif. 90406

Deputy Director and Chief Scientist
Office of Naval Research Branch Office
1030 East Green Street
Pasadena, California 91101

Aeronautics Library
Graduate Aeronautical Laboratories
California Institute of Technology
1201 E. California Blvd.
Pasadena, California 91109

Professor Nicholas George
California Institute of Technology
Pasadena, California 91109

Commanding Officer
Naval Weapons Center
Corona Laboratories
Attn: Library
Corona, California 91720

Dr. F. R. Charvat
Union Carbide Corporation
Materials Systems Div., Crystal Products
Dept., 8888 Balboa Avenue
P.O. Box 23017
San Diego, Calif. 92123

Hollander Associates
P.O. Box 2276
Fullerton, California 92633

Commander, U.S. Naval Missile Center
(56322)
Point Mugu, California 93041

W. A. Eberspacher, Associate Head
Systems Integration Division
Code 5340A, Box 15
U.S. Naval Missile Center
Point Mugu, California 93041

Sciences-Engineering Library
University of California
Santa Barbara, California 93106

Commander (Code 753)
Naval Weapons Center
Attn: Technical Library
China Lake, California 93555

Library (Code 2124)
Technical Report Section
Naval Postgraduate School
Monterey, California 93940

Glen A. Myers (Code 52Mv)
Assoc. Professor of Elec. Engineering
Naval Postgraduate School
Monterey, California 93940

Dr. Leo Young
Stanford Research Institute
Menlo Park, Calif. 94025

Lenkurt Electric Co., Inc.
1105 County Road
San Carlos, California 94070
Attn: Mr. E. K. Peterson

Director
Microwave Laboratory
Stanford University
Stanford, California 94305

Director
Stanford Electronics Laboratories
Stanford University
Stanford, California 94305

Director, Electronics Research
Laboratory
University of California
Berkeley, California 94720

Security Classification

DOCUMENT CONTROL DATA - R & D

(Security classification of title, body of abstract and indexing annotation must be entered when the overall report is classified)

1. ORIGINATING ACTIVITY *(Corporate author)*

Coordinated Science Laboratory
University of Illinois
Urbana, Illinois 61801

2a. REPORT SECURITY CLASSIFICATION

UNCLASSIFIED

2b. GROUP

3. REPORT TITLE

MULTIPLE STATES AND VARIABLE INTENSITY IN THE PLASMA DISPLAY PANEL

4. DESCRIPTIVE NOTES *(Type of report and inclusive dates)*

5. AUTHOR(S) *(First name, middle initial, last name)*

William Dooley Petty

6. REPORT DATE	7a. TOTAL NO. OF PAGES	7b. NO. OF REFS
November, 1970	74	None

8a. CONTRACT OR GRANT NO.

DAAB-07-67-C-0199

b. PROJECT NO.

N2269-69-C-0013

Owens-Illinois, Incorporated

c.

d.

9a. ORIGINATOR'S REPORT NUMBER(S)

R-497

9b. OTHER REPORT NO(S) *(Any other numbers that may be assigned this report)*

UILU-ENG 70-242

10. DISTRIBUTION STATEMENT

This document has been approved for public release and sale; its distribution is unlimited.

11. SUPPLEMENTARY NOTES

12. SPONSORING MILITARY ACTIVITY

Joint Services Electronics Program through U. S. Army Electronics Command; NADC; ARPA

13. ABSTRACT

In its normal operation the plasma panel exhibits a bistable range in which the cells can exist in either of two stable modes. The "on" state results from a discharge every half cycle, and the "off" state corresponds to no discharges. This investigation is concerned with the attainment of multiple stable states with corresponding multiple intensities. The application of this technology is related most directly to computer output displays where the inherent memory of the multiple states is desirable.

DD FORM 1 NOV 65 1473

Security Classification

14. KEY WORDS	LINK A		LINK B		LINK C	
	ROLE	WT	ROLE	WT	ROLE	WT
Plasma Display Panel						
Display Grey Scale						
Digital Display						